

AC Josephson Signatures of the Superconducting Higgs/Amplitude Mode

Aritra Lahiri,^{1,*} Sang-Jun Choi,² and Björn Trauzettel^{1,3}

¹*Institute for Theoretical Physics and Astrophysics,
University of Würzburg, D-97074 Würzburg, Germany*

²*Department of Physics Education, Kongju National University, Gongju 32588, Republic of Korea*

³*Würzburg-Dresden Cluster of Excellence ct.qmat, Germany*

(Dated: September 20, 2024)

The Higgs mode in superconductors corresponds to oscillations of the amplitude of the order parameter. While its detection typically entails resonant optical excitation, we present a purely transport-based setup wherein it is excited in a voltage biased Josephson junction. Demonstrating the importance of order parameter dynamics, the interplay of Higgs resonance and Josephson physics enhances the second harmonic Josephson current oscillating at twice the usual Josephson frequency in transparent junctions featuring single-band s-wave superconductors. If the leads have unequal equilibrium superconducting gaps, this second harmonic component may even eclipse its first harmonic counterpart, thus furnishing a unique hallmark of the Higgs oscillations.

The non-equilibrium dynamics of superconductors (SCs), resulting from an interplay of collective modes and quasiparticles, have been studied extensively [1–3]. Recent experimental developments [4–10] have ushered in several insights, especially about the superconducting Higgs mode [7–17]. The spontaneous $U(1)$ symmetry breaking in SCs results in a complex order parameter $\Delta(t) = |\Delta(t)| \exp(i\theta(t))$ with two collective modes: Higgs mode, corresponding to the amplitude $|\Delta(t)|$, and Goldstone mode, tied to the phase $\theta(t)$. While the Goldstone mode is pushed up to the plasma frequency [18], the Higgs mode has energy $\omega_H = 2\Delta_0$ [13, 14], where Δ_0 is the equilibrium gap amplitude. Being a scalar mode with no charge [14, 19], it has no linear coupling to the electromagnetic field. As such, its detection requires either strong lasers to harness non-linear electromagnetic effects made possible only by recent advances in THz technology [7–10, 16, 17, 20–22], or coupling with coexisting electronic orders such as charge-density waves [23–26]. Departing from this paradigm of purely optical techniques, there are limited transport-based proposals [27–35].

In this Letter, we investigate the Higgs mode in transparent voltage-biased Josephson junctions without external irradiation. The Josephson effect [36] epitomises coherent phase dynamics, with the interference of SC condensates at the junction generating a supercurrent. For a constant voltage V , in the absence of amplitude oscillations, a supercurrent $\sim \sin(\omega_J t)$ is generated solely by the condensate phase difference, where $\omega_J = 2eV$ ($\hbar = 1$) is the Josephson frequency. We find that the Josephson coupling induces OP amplitude oscillations by linking it to the energy emitted by tunneling Cooper pairs [37] via the Josephson phase difference [14, 38], obviating the need for external irradiation (see Fig. 1). Microscopically, the pairs coherently dissociate into Bogoliubov quasiparticles over the energy gap Δ_0 and recombine, requiring energy $\geq 2\Delta_0$. Consequently, a resonance emerges at $\omega_J = \omega_H$. While the possibility of probing the collective modes of a fluctuating superconductor slightly

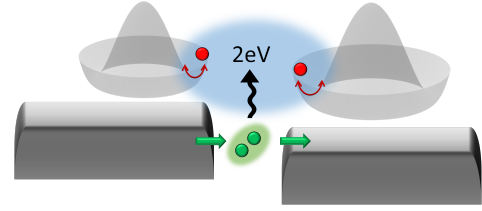


FIG. 1. Schematic of the Higgs mode, corresponding to radial oscillations of the OP (red balls) in the free-energy landscape (mexican hat). It is excited by radiating tunneling Cooper pairs (green balls) in a voltage-biased Josephson junction.

above its critical temperature using DC pair tunneling is established [39, 40], recently this was extended to zero temperature in a Josephson setup [34]. However, the Higgs mode was obfuscated by multiple Andreev reflections appearing at the same voltage in the DC current-voltage characteristics. We investigate instead the AC Josephson response, finding that the interplay of varying condensate phases and amplitudes generates a strong current at frequency $2\omega_J$. Remarkably, it can supercede the typical ω_J current when the leads' equilibrium gaps differ significantly, constituting a clear indication of Higgs oscillations in time-reversal symmetric Josephson junctions featuring single-band s-wave SCs [41–53].

Phenomenology.— For an intuitive picture, we start with the phenomenological zero-temperature effective field theory of the superconducting OP [13, 14, 19, 54–59]. On expanding about the equilibrium OP values, $\Delta_{L/R} = \Delta_{0,L/R} + \delta\Delta_{L/R}$, the Gaussian Lagrangian density is given by $\mathcal{L} = \sum_{j=L,R} \mathcal{L}_j + \mathcal{L}_J$, where,

$$\begin{aligned} \mathcal{L}_j &= (\partial_t \delta\Delta_j)^2 - \vartheta^2 (\partial_x \delta\Delta_j)^2 - \omega_{H,j}^2 \delta\Delta_j^2, \\ \mathcal{L}_J &= -2J\Delta_L\Delta_R \cos(\omega_J t). \end{aligned} \quad (1)$$

Here, $\Delta_{L/R} \in \mathfrak{R}$ are the OPs in the left/right leads, $\vartheta \sim$ Fermi velocity, and $J \sim \mathcal{T}^2$ where \mathcal{T} parametrises the coupling across the junction. We use a gauge where

the gaps are real, and the Josephson phase accounts for the voltage-dependent condensate phases. Particle-hole symmetry [13, 14, 60, 61] dictates the dynamical term $(\partial_t \delta \Delta)^2$. The Higgs mass $\omega_{H,L/R} = 2\Delta_{0,L/R}$ [13, 14, 54] results from microscopic calculations. The non-equilibrium OP corrections $\delta \Delta_{L/R}$ satisfy

$$\iint_{t',x'} \begin{bmatrix} \chi_{\Delta\Delta,L}^{-1} & s'_{\phi,L} \\ s'_{\phi,R} & \chi_{\Delta\Delta,R}^{-1} \end{bmatrix}_{(t',x';x',x')} \begin{bmatrix} \delta \Delta_L \\ \delta \Delta_R \end{bmatrix}_{(t';x')} = \begin{bmatrix} s_{\phi,L} \\ s_{\phi,R} \end{bmatrix}_{(t;x)} \quad (2)$$

with $\chi_{\Delta\Delta,L/R}^{-1} = (\partial_t^2 + \omega_{H,L/R}^2 - \vartheta^2 \partial_x^2) \delta(t-t') \delta(x-x')$, $s_{\phi,L/R} = -J \Delta_{0,R/L} \cos(\omega_J t) \delta(x)$, and $s'_{\phi,L/R} = J \cos(\omega_J t) \delta(t-t') \delta(x)$. Eq. (2) resembles driven coupled oscillators. The source term s_ϕ encapsulates the energy emitted by tunneling pairs. Thus, it oscillates at ω_J . The cross terms s'_ϕ describe the coupling between the oscillating OPs, which are driven by the junction field with s'_ϕ oscillating at ω_J . At leading order in J , neglecting the cross-coupling, $\delta \Delta_{L/R}^{(J)}(t) = \int_{-\infty}^t dt' \chi_{\Delta\Delta,L/R}(t,t') s_{\phi,L/R}(t')$. An explicit calculation for $\omega_J < \omega_{H,L/R}$ reveals $\delta \Delta_{L/R}(t,x) = (-J/2) \cos(\omega_J t) |\omega_J^2 - \omega_{H,L/R}^2|^{-1/2} \exp(-|\omega_J^2 - \omega_{H,L/R}^2|^{1/2} |x|/\vartheta^2)$, deriving its resonant enhancement from the Higgs pole in $\chi_{\Delta\Delta,L/R}(\omega_J, q) = 1/(-\omega_J^2 + \omega_{H,L/R}^2 + \vartheta^2 q^2)$. Within this simple model, the junction current may be approximated as $I \sim J \Delta_L(t) \Delta_R(t) \sin(\omega_J t)$. Note that it is sensitive to the time-dependence of the OP phases, as well as the amplitudes.

We discover that, for $\Delta_{0,L} \neq \Delta_{0,R}$, the Higgs oscillations in the OP manifest as a Josephson current with an enhanced $2\omega_J$ component, which may even dominate the usual ω_J component. Considering $\Delta_{0,L} < \Delta_{0,R}$ without loss of generality, as the voltage is increased and ω_J approaches $\omega_{H,L}$, $\delta \Delta_L$ is Higgs-enhanced while the non-resonant $\delta \Delta_R$ is small. In this regime, where $\Delta_L = \Delta_{0,L} + \delta \Delta_L$ and $\Delta_R \approx \Delta_{0,R}$, we find a $2\omega_J$ component in the current $I_{2\omega_J}$ bearing the amplitude $I_{2\omega_J} = I_{\omega_J} f_H$, where $I_{\omega_J} = J \Delta_{0,L} \Delta_{0,R}$ is the amplitude of the usual ω_J component, and $f_H = -(J/2)(\Delta_{0,R}/\Delta_{0,L}) |\omega_{H,L}^2 - \omega_J^2|^{-0.5}$ reflects the Higgs enhancement. At resonance, $I_{2\omega_J}$ is bounded only by the Higgs lifetime.

For equal equilibrium gaps $\Delta_{0,L} = \Delta_{0,R} = \Delta_0$, instead, both OPs reveal Higgs oscillations with $\delta \Delta_L = \delta \Delta_R$. A similar analysis shows in this case that while $I_{2\omega_J} = -J^2 \Delta_0^2 |\omega_H^2 - \omega_J^2|^{-0.5}$, even $I_{\omega_J} = J \Delta_0^2 (1 + (J^2/16) |\omega_H^2 - \omega_J^2|^{-1})$ is Higgs enhanced, where $\omega_H = 2\Delta_0$. This precludes a dominant $2\omega_J$ current.

Finally, despite the simplicity and intuitiveness of Eq. (1) with the Josephson term [14], $\mathcal{L}_J \sim \Delta_L(t) \Delta_R(t) \cos(\phi = \omega_J t)$, which can in fact be motivated from microscopic calculations (detailed in [62]), it is nevertheless an equilibrium formulation, applicable only approximately for *tunnel* junctions for sub-gap voltages, in

the absence of dissipative quasiparticle tunneling [67–69]. In the present scenario, where the OP oscillates at the same time scale as ϕ , it is imperative to account for the proper retarded dynamics [66, 67, 70, 71]. Furthermore, the phenomenological model is unable to account for the decay of the Higgs mode into the quasiparticle continuum [12], which is required for an accurate description of the regime with $\omega_J \gtrsim \omega_{H,L/R}$. The microscopic Keldysh approach employed in the remainder of the article is capable of handling these limitations.

Model.— We consider s-wave BCS superconducting Hamiltonians with attractive contact interaction [72–75]. Assuming specular tunneling and thus homogeneity (uniform OP) along the direction(s) transverse to current transport, we consider a single-channel Josephson junction, with leads $j = L/R$ (left/right) having $N_{1,L/R}$ sites, connected to infinite superconducting reservoirs. Our conclusions remain unchanged on considering multi-channel systems with a finite width [62, 76]. The mean-field action is $S = S_L + S_R + S_T$, where,

$$S_{L/R} = \sum_{j \in L/R, \sigma} \int_t (-\zeta c_{j+1\sigma}^\dagger c_{j\sigma} - \zeta c_{j\sigma}^\dagger c_{j+1\sigma}) + (\Delta_j(t) c_{j\sigma}^\dagger c_{j\sigma'}^\dagger + \Delta_j^*(t) c_{j\sigma'} c_{j\sigma}) + \frac{|\Delta_j(t)|^2}{g}, \quad (3)$$

and

$$S_T = \sum_\sigma \int_t -\mathcal{T} (e^{i\frac{\phi(t)}{2}} c_{LN_{1,L}\sigma}^\dagger c_{R1\sigma} + e^{-i\frac{\phi(t)}{2}} c_{R1\sigma}^\dagger c_{LN_{1,L}\sigma}). \quad (4)$$

Here, ζ is the hopping amplitude (bandwidth = 4ζ), $g > 0$ is the BCS attractive interaction, \mathcal{T} is the junction coupling which is independent of energy for voltages $\sim \Delta$ [77], and $\phi(t) = \int_{-\infty}^t d\tau 2eV(\tau)$ (second Josephson relation). We use a gauge which shifts the voltage into the junction coupling [78]. We assume that in the initial gauge the phase of the OP remains spatially uniform inside the leads, resulting in real values of $\Delta(t)$ following the gauge transformation. This typically holds when electric fields are restricted to the barrier region [79–82].

We use the Keldysh-Gorkov framework for a self-consistent solution to the OP [83–89]. With the lesser Green's function $G^<$ given by [83, 90–95],

$$G^< = G^r \Sigma^< G^a, \quad (5)$$

the non-equilibrium gap equation reads,

$$\Delta_j(t) = ig F_{j,j}^<(t, t), \quad (6)$$

where $F^<$ is the anomalous component of $G^<$.

Owing to the time-periodicity of Eq. (3) for DC voltage, we solve the Keldysh-Gorkov equations (5) and (6) by the Floquet technique [96–101]. The two-time Green's

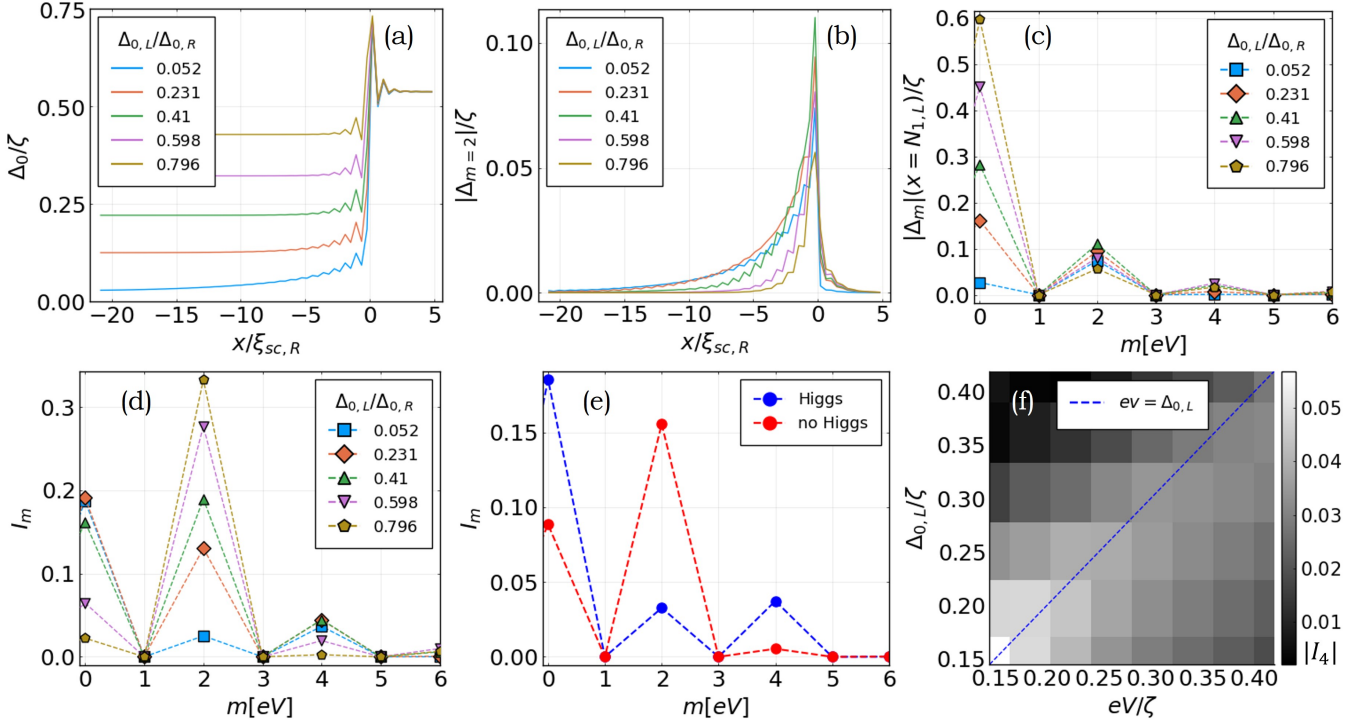


FIG. 2. Numerically obtained results for varying $\Delta_{0,L}$, with constant $\Delta_{0,R}$. We consider $\mu = 0$, $\mathcal{T} = 0.4\zeta$ (normal state transparency ≈ 0.48 [78]), $\Gamma = 0.075\zeta$, and $eV = 0.2\zeta$. $\xi_{sc,R} = 4\zeta/(\pi\Delta_{0,R})$ is the SC coherence length of the right SC (remains unchanged). $x < (>)0$ denotes the left(right) lead. (a) Equilibrium gap Δ_0 . (b) Δ_2 (frequency $\omega_J = 2(eV)$) spatially decaying over a length $\sim \xi_{sc,L}$. (c) Floquet components of the OP at the site immediately neighbouring the junction in the left lead ($x = N_{1,L}$). Recall, $\Delta_{m=0} = \Delta_0$, and $\Delta_{m \neq 0} = (1/T) \int (d\omega/(2\pi)) e^{im\Omega t} \delta\Delta(t)$. With decreasing $\Delta_{0,L}/\Delta_{0,R}$, Δ_2 (frequency $\omega_J = 2(eV)$) becomes relatively stronger than Δ_0 . (d) Floquet components of the current (arbitrary units). With decreasing $\Delta_{0,L}/\Delta_{0,R}$ the second-harmonic I_4 (frequency $2\omega_J = 4(eV)$) strengthens, eventually dominating the usual I_2 (frequency $\omega_J = 2(eV)$). (e) Current (blue) with and (red) without Higgs oscillations for $\Delta_{0,L}/\Delta_{0,R} = 0.052$. We force $\delta\Delta = 0$ in the latter. I_4 is larger than I_2 only with Higgs oscillations. (f) Amplitude of I_4 (frequency $2\omega_J = 4(eV)$) with varying voltage and $\Delta_{0,L}$, peaked at $eV \approx \Delta_{0,L}$. The slight deviation from $eV = \Delta_{0,L}$ likely stems from the enhancement of the equilibrium gap near the junction from its bulk value $\Delta_{0,L}$ (see panel (a)).

functions are expanded as

$$G_{ab}(t, t') = \sum_{m,n} \int_0^\Omega \frac{d\omega}{2\pi} e^{i(\omega+n\Omega)t' - i(\omega+m\Omega)t} G_{mn,ab}(\omega), \quad (7)$$

where $\Omega = 2\pi/T = eV$ is the fundamental Floquet frequency, the indices a, b denote the combined Nambu and spatial indices, and $G_{mn,ab}(\omega + l\Omega) = G_{(m+l)(n+l)}(\omega)$. The (Keldysh) Dyson equations become $G_{mn,ab}(\omega) = g_{mn,ab}(\omega) + \sum_{l,l'} g_{ml,ac}(\omega) \Sigma_{ll',cd}(\omega) G_{l'n,db}(\omega)$, where $g_{mn,ab}(\omega) = g_{ab}(\omega + m\Omega) \delta_{mn}$ is defined in the absence of tunneling. Following standard procedure [102], we partition the system into two leads connected at the Josephson junction which we treat exactly, and two spatially homogeneous semi-infinite reservoirs attached to the far-ends of the leads. The self-energy consists of four terms: (i) tunneling self energy $\Sigma_{T,RL,m-n}^{r/a} = \Sigma_{T,LR,n-m}^{r/a*} = -[V_{m-n}\tau_+ - V_{-m+n}^*\tau_-]$, where $V_{m-n} = (1/T) \int (d\omega/(2\pi)) e^{i(m-n)\Omega t} \mathcal{T} e^{-i\phi(t)/2}$, and $\tau_\pm = (\tau_0 \pm \tau_3)/2$ with τ_μ denoting the Pauli

matrices in Nambu space, (ii) OP self energy, $\Sigma_{\delta\Delta,m-n,ab}^{r/a} = [\Delta_{m-n}\tau_+ + \Delta_{n-m}^*\tau_-]$ for $m \neq n$, where $\Delta_{m-n \neq 0} = (1/T) \int (d\omega/(2\pi)) e^{i(m-n)\Omega t} \delta\Delta(t)$, (iii) reservoir self-energy, $\Sigma_{\text{res},L,m-n,ab}^{r/a/<} = \zeta^2 \tau_3 g_L \delta_{a,L1/RN_{1,R}} \delta_{b,L1/RN_{1,R}}$, where $L1/RN_{1,R}$ denote the lead sites immediately neighbouring the reservoir and g_L is the boundary Green's function [102], (iv) broadening self-energy $\Sigma_\Gamma^{r/a} = \pm i\Gamma/2$ and $\Sigma_\Gamma^< = -i\Gamma f(\omega)$, where $f(\omega)$ is the Fermi function. It aids numerical convergence, and accounts for the lifetime arising from, e.g., relaxation to the quasiparticle continuum, electron-phonon interaction, etc [71]. Following this prescription, the Floquet components of the current are obtained as [71, 78, 98, 101],

$$I_n = \sum_{l,m} e \int_0^\Omega \frac{d\omega}{2\pi} \text{Tr} [\tau_3 \Sigma_{T,LR,m+n-l}^< G_{R1LN_{1,l,m}}^<(\omega) - (L \leftrightarrow R)]. \quad (8)$$

Results.— The numerical solution to Eqs. (5) and (6)

is presented in Fig. 2. In Fig. 2 (a-c), for a given tunnel amplitude, we show that as the asymmetry in the equilibrium gaps increases, the OP oscillations at frequency ω_J in the lead with the smaller gap intensify near the junction, exceeding its equilibrium value. This occurs as the electrons previously forming static equilibrium gaps now contribute to the Higgs-oscillating pairs. Consequently, the second harmonic current at frequency $2\omega_J$ grows, as shown in Fig. 2(d). Eventually, for sufficiently small $\Delta_{0,L}/\Delta_{0,R}$ we obtain a transition when the $2\omega_J$ component starts dominating the usual ω_J component. Note that the strength of the $2\omega_J$ current is in direct correspondence with the Higgs resonance $eV = \Delta_{0,L}$, as revealed by Fig. 2 (f). We emphasise that the $2\omega_J$ current does not dominate in conventional single-band SCs with *time-constant* gaps [41–53]. This is corroborated by our numerical calculation in Fig. 2(e) where we compare the currents with and without the Higgs modulation $\delta\Delta_{L/R}$, while leaving $\Delta_{0,L/R}$ unchanged. Lastly, for a given set of equilibrium gaps, the OP oscillations and the $2\omega_J$ current grow with increasing junction coupling \mathcal{T} [62].

Complementing the phenomenological analysis, we motivate the numerical results with a microscopic perturbation theory. Starting with the bulk equilibrium gap Δ_0 , we write $\Delta(t, x) = \Delta_0 + \delta\Delta(t, x)$ for each lead. The corresponding self-energy is $\Sigma_{\delta\Delta}(t, x) = \delta\Delta(t, x)\tau_x$. The tunneling self energy is $\Sigma_{T,LR}(t) = \Sigma_{T,RL}^*(t) = (-\mathcal{T})\tau_z \exp(-i\phi(t)\tau_z/2)$. Using the Dyson equation, we obtain up to $\mathcal{O}(\mathcal{T}^3)$, $G_{L/R}^< = g_{L/R}^< + \sum_{j=1,2,3} \delta(G_{L/R}^<)^{(j)}$. Here, $\delta(G_{L/R}^<)^{(1)}$ has one instance of $\Sigma_{\delta\Delta}$, and accounts for the intrinsic dynamics of the pairs. It defines the Higgs susceptibility. $\delta(G_{L/R}^<)^{(2)}$ has two instances of Σ_T , and describes the effect of the radiating pairs tunneling across the junction. Finally, $\delta(G_{L/R}^<)^{(3)}$ has one instance of $\Sigma_{\delta\Delta}$ and two instances of Σ_T . It captures the cross-coupling between the OP oscillations of the two leads mediated by the tunneling pairs. As detailed in the SM [62], this expansion for $G^<$, along with Eq. (6), yields the microscopic version of the driven coupled oscillator model stated in Eq. (2) with susceptibility and sources given by

$$\begin{aligned} \chi_{\Delta\Delta,\alpha}^{-1}(r, r') &= \frac{\delta(r - r')}{g} + \frac{\Im\text{tr}[\tau_1(g_\alpha(r, r') \cdot \tau_1 \cdot g_\alpha(r', r))^{<}]}{2}, \\ s_{\phi,\alpha}(r) &= - \frac{\left[\Im\text{tr}[\tau_1(g_\alpha(r, r_1) \cdot \Sigma_{T,\alpha\alpha'}(r_1) \cdot g_{\alpha'}(r_1, r_2) \cdot \Sigma_{T,\alpha'\alpha}(r_2) \cdot g_\alpha(r_2, r))^{<}]} \right]}{2}, \\ s'_{\phi,\alpha}(r, r') &= \frac{\left[\Im\text{tr}[\tau_1(g_\alpha(r, r_1) \cdot \Sigma_{T,\alpha\alpha'}(r_1) \cdot g_{\alpha'}(r_1, r') \cdot \tau_1 \cdot g_{\alpha'}(r', r_2) \cdot \Sigma_{T,\alpha'\alpha}(r_2) \cdot g_\alpha(r_2, r'))^{<}]} \right]}{2}, \end{aligned} \quad (9)$$

where $\alpha, \alpha' = L/R$ denote the leads, $r \equiv (t; x)$, and \cdot denotes convolution in space and time with $r_{1,2}$ integrated over. Note that $\Sigma_T \neq 0$ only at $x = 0$.

The OP response is governed by $\chi_{\Delta\Delta}(\omega, q) =$

$[(1/g) + (1/2)\Im\chi_{\Delta\Delta,0}(\omega, q) - (i/2)\Re\chi_{\Delta\Delta,0}(\omega, q)]^{-1}$, where $\chi_{\Delta\Delta,0}(\omega, q) = \int \frac{d\bar{\omega}}{2\pi} \int \frac{d\bar{k}}{2\pi} \text{tr}[\tau_1(g_L(\bar{\omega} + \omega; \bar{k} + q)\tau_1 g_L(\bar{\omega}; \bar{k}))^{<}]$ is the pair correlation. Microscopically, $\chi_{\Delta\Delta}$ describes how tunneling processes and past OP variations propagate to affect the present OP. The resulting dynamics is governed by the singularity of $\chi_{\Delta\Delta}(\omega, q)$ at the Higgs frequency $\omega_H(q)$, with $\omega_H(q = 0) = 2\Delta_0$. Both source and cross-coupling terms are second order in tunneling and oscillate at the Josephson frequency $2eV$, as each tunnel process provides energy eV . Hence, the OP is resonantly excited when the radiated pair energy $2eV$ matches ω_H . We elaborate on the details in the SM [62], and show numerically obtained results for $\Re\chi_{\Delta\Delta}^{-1}(\omega, q)$ and s_ϕ , in Fig. 3.

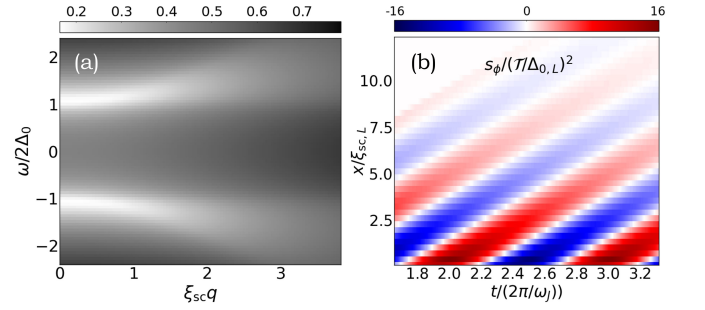


FIG. 3. (a) $\Re\chi_{\Delta\Delta}^{-1}(\omega, q) = \zeta(\frac{1}{g} + \frac{1}{2}\Im\chi_{\Delta\Delta,0}(\omega, q))$ for a three-dimensional s-wave SC, showing a dip at the Higgs frequency $\omega_H(q)$. We use $\zeta = 10\Delta_0$, $\mu = 0$, $\Gamma = 0.1\Delta_0$, and $\xi_{sc} = 4\zeta/(\pi\Delta_0)$ is the coherence length. (b) $s_\phi/(\mathcal{T}/\Delta_{0,L}^2)$ for $\zeta = 10\Delta_{0,L}$, $\mu = 0$, $\Gamma = 0.25\Delta_{0,L}$ and $\Delta_{0,R} = 5\Delta_{0,L}$. It oscillates at ω_J , and decays into the lead ($x > 0$) over a few $\xi_{sc,L}$.

Discussion.— We propose the excitation and detection of the Higgs mode in SCs using the AC Josephson effect without external irradiation. In asymmetric junctions [103–108] having sufficiently different equilibrium gaps, which may be tuned experimentally [108, 109], along with high transparency, the second Josephson harmonic oscillating at twice the usual AC Josephson frequency dominates the current. As such, it may be readily observed, for instance, in the Josephson radiation [110–112]. Ideally, we seek wide specular junctions to ensure that all transport channels/subbands experience the Higgs resonance effects [34], along with an atomically thin barrier and low environmental electromagnetic absorption [110, 112] at frequencies comparable to the smaller superconducting gap to ensure maximal Higgs excitation. Remarkably, our results are robust to the presence of Dynes broadening, for which we have used values as large as $\Gamma/\Delta_0 \sim 0.15$, while typical experimentally relevant values are $\Gamma/\Delta_0 \sim 10^{-3} - 10^{-1}$ [113, 114]. Furthermore, recent studies have shown that weak paramagnetic impurities (scattering rate $1/\tau_p \ll \Delta_0$) can push the Higgs mode below the quasiparticle continuum [89, 115], thereby suppressing its decay and en-

hancing its signatures. Several experiments [116–119] have already reported a disproportionately large second harmonic Josephson current, while pointing at non-equilibrium dynamics.

This work was supported by the Würzburg-Dresden Cluster of Excellence `ct.qmat`, EXC2147, project-id 390858490, and the DFG (SFB 1170). We thank the Bavarian Ministry of Economic Affairs, Regional Development and Energy for financial support within the High-Tech Agenda Project “Bausteine für das Quanten Computing auf Basis topologischer Materialien”. The authors gratefully acknowledge the scientific support and HPC resources provided by the Erlangen National High Performance Computing Center (NHR@FAU) of the Friedrich-Alexander-Universität Erlangen-Nürnberg (FAU) under the NHR project b169cb. NHR funding is provided by federal and Bavarian state authorities. NHR@FAU hardware is partially funded by the German Research Foundation (DFG) – 440719683.

* aritra.lahiri@uni-wuerzburg.de

- [1] J.-J. Chang, and D. Scalapino, Nonequilibrium superconductivity. *J. Low Temp. Phys.* **31**, 1–32 (1978).
- [2] N. Kopnin, *Theory of Nonequilibrium Superconductivity* (Oxford University Press, New York, 2001).
- [3] M. Tinkham, *Non-Equilibrium Superconductivity in Festkörperprobleme (Advances in Solid State Physics, Vol. XIX)*, J. Treusch, ed. (Vieweg Braunschweig, 1979), p. 363.
- [4] D. Fausti, R. I. Tobey, N. Dean, S. Kaiser, A. Dienst, M. C. Hoffmann, S. Pyon, T. Takayama, H. Takagi, and A. Cavalleri, *Science* **331**, 189 (2011).
- [5] M. Mitrano, A. Cantaluppi, D. Nicoletti, S. Kaiser, A. Perucchi, S. Lupi, P. Di Pietro, D. Pontiroli, M. Riccò, S. R. Clark, D. Jaksch, and A. Cavalleri, *Nature* **530**, 461 (2016).
- [6] F. Giorgianni, T. Cea, C. Vicario, C. P. Hauri, W. K. Withanage, X. Xi, and L. Benfatto, *Nat. Phys.* **15**, 341–346 (2019).
- [7] R. Matsunaga and R. Shimano, *Phys. Rev. Lett.* **109**, 187002 (2012).
- [8] R. Matsunaga, Y. I. Hamada, K. Makise, Y. Uzawa, H. Terai, Z. Wang, and R. Shimano, *Phys. Rev. Lett.* **111**, 057002 (2013).
- [9] M. Beck, I. Rousseau, M. Klammer, P. Leiderer, M. Mitterdorff, S. Winnerl, M. Helm, G. N. Gol’tsman, and J. Demsar, *Phys. Rev. Lett.* **110**, 267003 (2013).
- [10] R. Matsunaga, N. Tsuji, H. Fujita, A. Sugioka, K. Makise, Y. Uzawa, H. Terai, Z. Wang, H. Aoki, and R. Shimano, *Science* **345**, 1145 (2014).
- [11] P. W. Higgs, *Phys. Rev. Lett.* **13**, 508 (1964).
- [12] P. B. Littlewood and C. M. Varma, *Phys. Rev. B* **26**, 4883 (1982).
- [13] C. Varma, *J. Low. Temp. Phys.* **126**, 901 (2002).
- [14] D. Pekker and C. Varma, *Annu. Rev. Condens. Matter Phys.* **6**, 269 (2015).
- [15] R. Shimano and N. Tsuji, *Ann. Rev. Condens. Matter Phys.* **11**, 103 (2020).
- [16] R. Matsunaga, N. Tsuji, K. Makise, H. Terai, H. Aoki, and R. Shimano, *Phys. Rev. B* **96**, 020505(R) (2017).
- [17] K. Katsumi, N. Tsuji, Y. I. Hamada, R. Matsunaga, J. Schneeloch, R. D. Zhong, G. D. Gu, H. Aoki, Y. Gallais, and R. Shimano, *Phys. Rev. Lett.* **120**, 117001 (2018).
- [18] P. W. Anderson, *Phys. Rev.* **110**, 827 (1958).
- [19] L. Schwarz, PhD thesis, Freie Universität Berlin (2020).
- [20] D. Sherman, U. S. Pracht, B. Gorshunov, S. Poran, J. Jesudasan, M. Chand, P. Raychaudhuri, M. Swanson, N. Trivedi, A. Auerbach, et al., *Nat. Phys.* **11**, 188 (2015).
- [21] H. Chu, M.-J. Kim, K. Katsumi, S. Kovalev, R. D. Dawson, L. Schwarz, N. Yoshikawa, G. Kim, D. Putzky, Z. Z. Li, et al., *Nat. Commun.* **11**, 1793 (2020).
- [22] C. Vaswani, J. Kang, M. Mootz, L. Luo, X. Yang, C. Sundahl, D. Cheng, C. Huang, R. H. Kim, Z. Liu, et al., *Nat. Commun.* **12**, 258 (2021).
- [23] R. Sooryakumar, and M. V. Klein, *Phys. Rev. Lett.* **45**, 660 (1980).
- [24] M.-A. Méasson, Y. Gallais, M. Cazayous, B. Clair, P. Rodière, L. Cario, and A. Sacuto, *Phys. Rev. B* **89**, 060503(R) (2014).
- [25] T. Cea and L. Benfatto, *Phys. Rev. B* **90**, 224515 (2014).
- [26] R. Grasset, T. Cea, Y. Gallais, M. Cazayous, A. Sacuto, L. Cario, L. Benfatto, and M.-A. Méasson, *Phys. Rev. B* **97**, 094502 (2018).
- [27] M. A. Silaev, R. Ojajärvi, and T. T. Heikkilä, *Phys. Rev. Res.* **2**, 033416 (2020).
- [28] G. Tang, W. Belzig, U. Zülicke, and C. Bruder, *Phys. Rev. Research* **2**, 022068 (2020).
- [29] P. Vallet and J. Cayssol, *Phys. Rev. B* **108**, 094515 (2023).
- [30] V. Plastovets, A. S. Mel’nikov, and A. I. Buzdin, *Phys. Rev. B* **108**, 104507 (2023).
- [31] M. Heckschen and B. Sothmann, *Phys. Rev. B* **105**, 045420 (2022).
- [32] P. Derendorf, A. F. Volkov, and I. M. Eremin, *Phys. Rev. B* **109**, 024510 (2024).
- [33] T. Kuhn, B. Sothmann, J. Cayao, arXiv preprint arXiv:2312.13785 (2023).
- [34] P. A. Lee and J. F. Steiner, *Phys. Rev. B* **108**, 174503 (2023).
- [35] P. Vallet and J. Cayssol, *Phys. Rev. B* **110**, 024517 (2024).
- [36] B. D. Josephson, *Phys. Lett.* **1**, 7, 251–253 (1962).
- [37] M. Hofheinz, F. Portier, Q. Baudouin, P. Joyez, D. Vion, P. Bertet, P. Roche, and D. Esteve *Phys. Rev. Lett.* **106**, 217005 (2011).
- [38] T. Klapwijk, G. Blonder and M. Tinkham, *Physica B + C* **109**, 1657–1664 (1982).
- [39] R. A. Ferrell, *J. Low Temp. Phys.* **1**, 423 (1969).
- [40] D. J. Scalapino, *Phys. Rev. Lett.* **24**, 1052 (1970).
- [41] In time-reversal symmetric single-band s-wave SCs, the $2\omega_J$ component is smaller than the ω_J component, unless we have ferromagnetic components, spin-orbit interaction in the presence of a magnetic field, d- and p-wave SCs, and multiband SCs [42–53].
- [42] H. Sellier, C. Baraduc, F. Lefloch and R. Calemczuk, *Phys. Rev. Lett.* **92**, 257005 (2004).
- [43] H. Sickinger, A. Lipman, M. Weides, R. G. Mints, H. Kohlstedt, D. Koelle, R. Kleiner and E. Goldobin, *Phys. Rev. Lett.* **109**, 107002 (2012).
- [44] E. Goldobin, D. Koelle, R. Kleiner and A. Buzdin, *Phys. Rev. B* **76**, 224523 (2007).
- [45] S. M. Frolov, D. J. Van Harlingen, V. V. Bolginov, V.

- A. Oboznov, and V. V. Ryazanov, Phys. Rev. B **74**, 020503(R) (2006).
- [46] F. Li, L. Wu, L. Chen, S. Zhang, W. Peng, and Z. Wang, Phys. Rev. B **99**, 100506(R) (2019).
- [47] T. Yokoyama, M. Eto, and Y. V. Nazarov, Phys. Rev. B **89**, 195407 (2014).
- [48] Y. Tanaka and S. Kashiwaya, Phys. Rev. B **56**, 892 (1997).
- [49] T. K. Ng, and N. Nagaosa, EPL **87**, 17003 (2009).
- [50] Y. Asano, Y. Tanaka, M. Sigrist, and S. Kashiwaya, Physical Review B **67**, 184505 (2003).
- [51] C. J. Trimble, M. T. Wei, N. F. Q. Yuan, S. S. Kalantre, P. Liu, H.-J. Han, M.-G. Han, Y. Zhu, J. J. Cha, L. Fu, and J. R. Williams, npj Quantum Materials **6**, 61 (2021).
- [52] O. Can, T. Tummuru, R. P. Day, I. Elfmov, A. Damaschelli, and M. Franz, Nature Physics **17**, 519 (2021).
- [53] T. Tummuru, S. Plugge, and M. Franz, Phys. Rev. B **105**, 064501 (2022).
- [54] H. Kleinert, Collective Classical and Quantum Fields: In Plasmas, Superconductors, Superfluid 3 He, and Liquid Crystals (World Scientific, Singapore, 2018).
- [55] A. van Otterlo, D. S. Golubev, A. D. Zaikin, and G. Blatter, Eur. Phys. J. B **10**, 131 (1999).
- [56] N. Tsuji and H. Aoki, Phys. Rev. B **92**, 064508 (2015).
- [57] T. H. Hansson, V. Oganesyan, and S. L. Sondhi, Annals of Physics **313**, 497 (2004).
- [58] L. Schwarz, R. Haenel, and D. Manske, Phys. Rev. B **104**, 174508 (2021).
- [59] R. Haenel, P. Froese, D. Manske, and L. Schwarz, Phys. Rev. B **104**, 134504 (2021).
- [60] Typically realised in weak-coupling SCs in the high density limit $\Delta \ll \mu$, when the variation of the normal-state density of states in the vicinity of the Fermi-level upto an energy range $\sim \Delta$ is negligible [61].
- [61] D. Phan and A. V. Chubukov Physical Review B **107**, 134519 (2023).
- [62] See Supplemental Material, which includes Refs. [63–65], containing numerical results for varying junction coupling, bandwidth, and transverse subbands, as well as details of the perturbative analysis.
- [63] J. C. Cuevas and A. L. Yeyati, Phys. Rev. B **74**, 180501 (2006).
- [64] J. C. Cuevas and E. Scheer, Molecular Electronics: An Introduction To Theory And Experiment (World Scientific, Singapore, 2010).
- [65] A. Barone and G. Paterno, Physics and Applications of the Josephson Effect (Wiley, New York, 1982).
- [66] A. I. Larkin and Y. N. Ovchinnikov, Zh. Eksp. Teor. Fiz. **51**, 1535 [Sov. Phys. JETP **24**, 1035 (1967)].
- [67] V. Ambegaokar, U. Eckern, and G. Schön, Phys. Rev. Lett. **48**, 1745 (1982).
- [68] U. Eckern, G. Schön, and V. Ambegaokar, Phys. Rev. B **30**, 6419 (1984).
- [69] G. Schön and A. D. Zaikin, Phys. Rep. **198**, 237 (1990).
- [70] N. R. Werthamer, Phys. Rev. **147**, 255 (1966).
- [71] A. Lahiri, S.-J. Choi, and B. Trauzettel, Phys. Rev. Lett. **131**, 126301 (2023).
- [72] A. A. Abrikosov, L. P. Gorkov, and I. E. Dzyaloshinski, Methods of Quantum Field Theory in Statistical Physics (Dover, New York, 1975).
- [73] P. G. de Gennes, Superconductivity of Metals and Alloys (Benjamin, New York, 1966).
- [74] G. Stefanucci, E. Perfetto and M. Cini, J. Phys.: Conf. Ser. **220** 012012 (2010).
- [75] A. Levy Yeyati, A. Martín-Rodero, and F. J. García-Vidal, Phys. Rev. B **51**, 3743 (1995).
- [76] Assuming a uniform OP along the cross-section $\Delta(t, x, y, z) = \Delta(t, x)$, the Hamiltonian splits into disjoint single-channel subblocks $H = \oplus_{k_y, k_z} H(x, k_y, k_z)$. The OP response from each subband/channel is in-phase in time domain. Thus, the full multi-subband solution differs only quantitatively from the numerically tractable single-channel simulation. We confirm this in the SM [62], considering planar junctions with finite widths.
- [77] J. C. Cuevas, J. Heurich, A. Martín-Rodero, A. Levy Yeyati, and G. Schön, Phys. Rev. Lett. **88**, 157001 (2002).
- [78] J. C. Cuevas, A. Martín-Rodero, and A. Levy Yeyati, Phys. Rev. B **54**, 7366 (1996).
- [79] S. N. Artemenko and A. G. Kobelkov, Phys. Rev. Lett. **78**, 3551 (1997).
- [80] T. Y. Hsiang and J. Clarke, Phys. Rev. B **21**, 945 (1980).
- [81] T. J. Rieger, D. J. Scalapino, and J. E. Mercereau, Phys. Rev. Lett. **27**, 1787 (1971).
- [82] K. V. Kulikov, M. Nashaat and Yu. M. Shukrinov, EPL **127** 67004 (2019).
- [83] H. P. Ojeda Collado, G. Usaj, J. Lorenzana, and C. A. Balseiro, Phys. Rev. B **99**, 174509 (2019).
- [84] A. Kamenev, Field Theory of Non-Equilibrium Systems (Cambridge University Press, Cambridge, England, 2011).
- [85] M. P. Kemoklidze and L. P. Pitaevskii, Zh. Eksp. Teor. Fiz. **50**, 243 (1966) [Sov. Phys. JETP **23**, 160 (1966)].
- [86] A. F. Volkov and S. M. Kogan, Zh. Eksp. Teor. Fiz. **65**, 2038, (1974) [Sov. Phys. JETP, **38**, 1018 (1974)].
- [87] V. L. Vadimov, I. M. Khaymovich, and A. S. Mel'nikov, Phys. Rev. B **100**, 104515 (2019).
- [88] T. Kuhn, B. Sothmann, and J. Cayao, Phys. Rev. B **109**, 134517 (2024).
- [89] M. Dzero, Phys. Rev. B **109**, L100503 (2024).
- [90] A.-P. Jauho, N. S. Wingreen, and Y. Meir Phys. Rev. B **50**, 5528 (1994).
- [91] Tianrui Xu, Takahiro Morimoto, Alessandra Lanzara and Joel E. Moore, Phys. Rev. B **99**, 035117 (2019).
- [92] L. V. Keldysh, Sov. Phys. JETP **20**, 1018 (1964)
- [93] G. Stefanucci and R. van Leeuwen, *Nonequilibrium Many-Body Theory of Quantum Systems: A Modern Introduction*, Cambridge University Press, Cambridge, (2013).
- [94] S. A. González, L. Melischek, O. Peters, K. Flensberg, K. J. Franke, and F. von Oppen, Phys. Rev. B **102**, 045413 (2020).
- [95] $G^< = (1 + \Sigma^r G^r) g^< (1 + G^a \Sigma^a) + G^r \Sigma^< G^a$. The first term refers to the initial conditions. In the presence of a finite lifetime $\sim 1/\Gamma$, it decays to zero before the bias voltage is applied due to the exponentially decaying $G^{r/a}$ [92–94].
- [96] D. F. Martinez, Journal of Physics A: Mathematical and General **36**, 9827 (2003).
- [97] G. Stefanucci, S. Kurth, A. Rubio, and E. K. U. Gross, Phys. Rev. B **77**, 075339 (2008).
- [98] L. P. Gavensky, G. Usaj, and C. A. Balseiro, Phys. Rev. B **103**, 024527 (2021).
- [99] P. San-Jose, J. Cayao, E. Prada and R. Aguado, New J. Phys. **15**, 075019 (2013).
- [100] C. J. Bolech and T. Giamarchi, Phys. Rev. B **71**, 024517 (2005).
- [101] L. P. Gavensky, PhD thesis, Instituto Balseiro - Universidad Nacional de Cuyo, Bariloche (2022).
- [102] M. P. Samanta and S. Datta, Phys. Rev. B **57**, 10972

- (1998).
- [103] J. S. Tsai, Y. Kubo, and J. Tabuchi, *Phys. Rev. Lett.* **58**, 1979 (1987).
- [104] Z. Z. Li, Y. Xuan, H. J. Tao, Z. A. Ren, G. C. Che, B. R. Zhao, and Z. X. Zhao, *Supercond. Sci. Technol.* **14**, 944 (2001).
- [105] X. Zhang, Y. S. Oh, Y. Liu, L. Yan, K. H. Kim, R. L. Greene, and I. Takeuchi, *Phys. Rev. Lett.* **102**, 147002 (2009).
- [106] M. Ternes, W.-D. Schneider, J.-C. Cuevas, C. P. Lutz, C. F. Hirjibehedin, and A. J. Heinrich, *Phys. Rev. B* **74**, 132501 (2006).
- [107] G. Germanese, F. Paolucci, G. Marchegiani, A. Braggio and F. Giazotto, *Nat. Nanotechnol.* **17**, 1084–1090 (2022).
- [108] G. Marchegiani, L. Amico, and G. Catelani, *PRX Quantum* **3**, 040338 (2022).
- [109] Y. Ivry, C.-S. Kim, A. E. Dane, D. De Fazio, A. N. McCaughan, K. A. Sunter, Q. Zhao, and K. K. Berggren, *Phys. Rev. B* **90**, 214515 (2014).
- [110] R. S. Deacon, J. Wiedenmann, E. Bocquillon, F. Domínguez, T.M. Klapwijk, P. Leubner, C. Brüne, E.M. Hankiewicz, S. Tarucha, K. Ishibashi, H. Buhmann, and L.W. Molenkamp. *Phys. Rev. X* **7**, 021011 (2017)
- [111] D. Laroche, D. Bouman, D. J. van Woerkom, A. Proutski, C. Murthy, D. I. Pikulin, C. Nayak, R. J. J. van Gulik, J. Nygård, P. Krogstrup, L. P. Kouwenhoven, and A. Geresdi, *Nat. Commun.* **10**, 245 (2019).
- [112] W. Liu, S. U. Piatrusha, X. Liang, S. Upadhyay, L. Furst, C. Gould, J. Kleinlein, H. Buhmann, M. P. Stehno, L. W. Molenkamp, arXiv:2408.06119 (2024).
- [113] R. C. Dynes, V. Narayanamurti, and J. P. Garno, *Phys. Rev. Lett.* **41**, 1509 (1978).
- [114] R. C. Dynes, J. P. Garno, G. B. Hertel, and T. P. Orlando, *Phys. Rev. Lett.* **53**, 2437 (1984).
- [115] Y. Li, M. Dzero, *Phys. Rev. B* **109**, 054520 (2024).
- [116] K. W. Lehnert, N. Argaman, H.-R. Blank, K. C. Wong, S. J. Allen, E. L. Hu, and H. Kroemer, *Phys. Rev. Lett.* **82**, 1265–1268 (1999).
- [117] R. C. Dinsmore III, M.-H. Bae, and A. Bezryadin, *Appl. Phys. Lett.* **93**, 192505 (2008).
- [118] P. Zhang, A. Zarassi, L. Jarjat, V. V. de Sande, M. Pendharkar, J. S. Lee, C. P. Dempsey, A. P. McFadden, S. D. Harrington, J. T. Dong, H. Wu, A. H. Chen, M. Heccevar, C. J. Palmstrøm, and S. M. Frolov, arXiv preprint arXiv:2211.07119 (2022).
- [119] A. Iorio, A. Crippa, B. Turini, S. Salimian, M. Carrega, L. Chirulli, V. Zannier, L. Sorba, E. Strambini, F. Giazotto, and S. Heun, *Phys. Rev. Res.* **5**, 033015 (2023).

Supplemental Material: AC Josephson Signatures of the Superconducting Higgs/Amplitude Mode

In this Supplemental Material, we present: (S1) A perturbative analysis deriving the Higgs susceptibility and source term, and establishing the qualitative equivalence between the microscopic Keldysh model which we use for our numerical calculations and the simple toy model in the introduction of the main text. (S2) Additional numerical results to show the effect of varying junction coupling, bandwidth, and device width/transverse modes.

CONTENTS

S1. Perturbative analysis	2
A. Dyson equation for $G^<$	2
B. Coupled oscillator correspondence	2
C. Non-equilibrium order parameter	2
D. Susceptibility	3
E. Source	6
F. Current	6
S2. Numerical analysis	7
A. Varying junction coupling	7
B. Varying hopping/bandwidth	7
C. Varying number of transverse modes/sub-bands: Planar specular junctions	9
References	11

S1. PERTURBATIVE ANALYSIS

A. Dyson equation for $G^<$

$$\begin{aligned}
(\delta G_L^<)^{(1)} &= (g_L \cdot \Sigma_{\delta\Delta_L} \cdot g_L)^< = (g_L^r \cdot \Sigma_{\delta\Delta_L} \cdot g_L^< + g_L^< \cdot \Sigma_{\delta\Delta_L} \cdot g_L^a), \\
(\delta G_L^<)^{(2)} &= (g_L \cdot \Sigma_{T,LR} \cdot g_R \cdot \Sigma_{T,RL} \cdot g_L)^< = \sum_{\substack{l_{1..3}=\{<aa, \\ r<a, rrr<\}}} g_L^{l_1} \cdot \Sigma_{T,LR} \cdot g_R^{l_2} \cdot \Sigma_{T,RL} \cdot g_L^{l_3}, \\
(\delta G_L^<)^{(3)} &= (g_L \cdot \Sigma_{T,LR} \cdot g_R \cdot \Sigma_{\delta\Delta_R} \cdot g_R \cdot \Sigma_{T,RL} \cdot g_L)^< = \sum_{\substack{m_{1..4}= \\ \{<aaa, r<aa, \\ rrr<a, rrrr<\}}} g_L^{m_1} \cdot \Sigma_{T,LR} \cdot g_R^{m_2} \cdot \Sigma_{\delta\Delta_R} \cdot g_R^{m_3} \cdot \Sigma_{T,RL} \cdot g_L^{m_4},
\end{aligned} \tag{S1}$$

where the lowercase letter denotes the bare Green's functions, and the products are convolutions in space and time. The second equality in each line follows from the Langreth rules.

B. Coupled oscillator correspondence

From Eq. (6), $\Delta_j(t) = igF_{j,j}^<(t, t)$, we collect the first three leading terms in \mathcal{T} ,

$$\begin{aligned}
\Delta_{0,L}(t, x) + \delta\Delta_L(t, x) &= \Re \frac{ig}{2} \text{tr}[\tau_1 G_L^<(t, t; x, x)] = \Re \frac{ig}{2} \text{tr}[\tau_1 g_L^<(t, t; x, x)] + \underbrace{\Re \frac{ig}{2} \text{tr}[\tau_1 \delta G_L^<(t, t; x, x)]}_{=\Delta_{0,L}} \\
\implies \frac{1}{g} \delta\Delta_L(t, x) &= \Re \frac{i}{2} \text{tr}[\tau_1 (g_L \cdot \Sigma_{\delta\Delta_L} \cdot g_L)^<(t, t; x, x)] + \Re \frac{i}{2} \text{tr}[\tau_1 (g_L \cdot \Sigma_{T,LR} \cdot g_R \cdot \Sigma_{T,RL} \cdot g_L)^<(t, t; x, x)] \\
&\quad + \Re \frac{i}{2} \text{tr}[\tau_1 (g_L \cdot \Sigma_{T,LR} \cdot g_R \cdot \Sigma_{\delta\Delta_R} \cdot g_R \cdot \Sigma_{T,RL} \cdot g_L)^<(t, t; x, x)]. \quad (\text{Using Eq. (S1)}) \tag{S2}
\end{aligned}$$

Note that by considering $\Sigma_{\delta\Delta} = \delta\Delta\tau_1$ we assume a real gap as mentioned in the main text. On rearranging, we recover Eq. (2) with the microscopic version of susceptibility and sources given by Eq. (9). In the following section, we obtain the expression for χ and elaborate on its essential features. We also obtain the behaviour of s_ϕ , which is plotted numerically in the main text. Their features qualitatively match those obtained from the phenomenological coupled-oscillator model in the section ‘‘Phenomenology’’ in the main text, thereby establishing the correspondence.

C. Non-equilibrium order parameter

Here we obtain the perturbative expression for the non-equilibrium variation in the OP. Considering a two-dimensional system (planar-junction) and assuming specular tunneling, starting with the equation for the non-equilibrium gap Eq. (2) and neglecting the cross-terms, we have,

$$\begin{aligned}
\frac{\delta\Delta_L(t; \{x, y\})}{g} &= -\frac{1}{2} \Im \int_{t_1} \sum_{x_1, y_1} \text{tr}[\tau_1 g_L(t, t_1; \{x, y\}, \{x_1, y_1\}) \tau_1 g_L(t_1, t; \{x_1, y_1\}, \{x, y\})]^< \delta\Delta(t_1; \{x_1, y_1\}) \\
&\quad - \frac{1}{2} \Im \iint_{t_1, t_2} \sum_{y_1, y_2} \text{tr}[\tau_1 g_L(t, t_1; \{x, y\}, \{0, y_1\}) \Sigma_{T,LR}(t_1) g_R(t_1, t_2; \{0, y_1\}, \{0, y_2\}) \Sigma_{T,RL}(t_2) g_L(t_2, t; \{0, y_2\}, \{x, y\})]^<.
\end{aligned} \tag{S3}$$

On Fourier transforming,

$$\begin{aligned} \frac{\sum_{\mathbf{q}}}{N_x N_y} \int \frac{d\omega}{(2\pi)} \frac{\delta\Delta_L(\omega; \mathbf{q})}{g} e^{-i\omega t + i\mathbf{q}\cdot\mathbf{r}} &= -\frac{1}{2} \Im \frac{\sum_{\mathbf{q}, \mathbf{k}_2}}{(N_x N_y)^2} \int \frac{d\omega}{(2\pi)} \frac{d\omega_2}{(2\pi)} \mathbf{tr} [\tau_1 g_L(\omega_2 + \omega; \mathbf{k}_2 + \mathbf{q}) \tau_1 g_L(\omega_2; \mathbf{k}_2)]^< \delta\Delta(\omega; \mathbf{q}) e^{-i\omega t + i\mathbf{q}\cdot\mathbf{r}} \\ &- \frac{1}{2} \Im \frac{\sum_{\substack{k_{1,x}, k_{2,x}, \\ k_{3,x}, k_{3,y}}}}{N_x^3 N_y} \int \frac{d\Omega_1 d\Omega_2 d\omega_3}{(2\pi)^3} \mathbf{tr} [\tau_1 g_L(\omega_3 + \Omega_1 + \Omega_2; k_{1,x}, k_{3,y}) \Sigma_{T,LR}(\Omega_1) g_R(\omega_3 + \Omega_2; k_{2,x}, k_{3,y}) \Sigma_{T,RL}(\Omega_2) g_L(\omega_3; k_{3,x}, k_{3,y})]^< \\ &e^{-i(\Omega_1 + \Omega_2)t + i(k_{1,x} - k_{3,x})x + ik_{3,y}y}, \end{aligned} \quad (\text{S4})$$

where we have considered specular tunneling, and $\Sigma_{T,LR/RL}(\Omega) = -\mathcal{T} \begin{bmatrix} \delta(\Omega \mp eV) & 0 \\ 0 & -\delta(\Omega \pm eV) \end{bmatrix}$.

Assuming transverse homogeneity, i.e., only the $q_y = 0$ component of the OP is non-zero, we obtain,

$$\delta\Delta(\omega; q_x, 0) = \chi_{\Delta\Delta,L}(\omega; q_x, 0) \frac{s_{\phi,L}(\omega; q_x, 0) - s_{\phi,L}^*(-\omega; -q_x, 0)}{2i}, \quad (\text{S5})$$

where

$$\chi_{\Delta\Delta,L}(\omega; q_x, 0) = \frac{1}{\frac{1}{g} + \frac{1}{2} \Im \frac{\sum_{\mathbf{k}_2}}{(N_x N_y)^2} \int \frac{d\omega_2}{(2\pi)} \mathbf{tr} [\tau_1 g_L(\omega_2 + \omega; \mathbf{k}_2 + q_x) \tau_1 g_L(\omega_2; \mathbf{k}_2)]^<}, \quad (\text{S6})$$

and

$$\begin{aligned} s_{\phi,L}(\omega; q_x, 0) &= -\frac{1}{2} \frac{\sum_{k_{2,x}, k_{3,x}}}{N_x^2} \int \frac{d\Omega_2 d\omega_3}{(2\pi)^2} \mathbf{tr} [\tau_1 g_L(\omega_3 + \omega; k_{3,x} + q_x, 0) \Sigma_{T,LR}(\omega - \Omega_2) g_R(\omega_3 + \Omega_2; k_{2,x}, 0) \Sigma_{T,RL}(\Omega_2) \\ &g_L(\omega_3; k_{3,x}, 0)]^<. \end{aligned} \quad (\text{S7})$$

Later, we convert the momentum sums $\frac{\sum_{k_x}}{N_x} \rightarrow \int \frac{dk_x}{2\pi}$, where k_x is the dimensionless product of the wavevector and the lattice constant. The source term in the numerator generates oscillations at ω_J (along with a DC renormalisation near the junction), with the magnitude of the OP governed by the singularities (corresponding to the Higgs mode in our case) of the susceptibility in the denominator. We show in the section on susceptibility that at the Higgs resonance, $\chi_{\Delta\Delta} \sim \sqrt{\Delta_{0,L}/\Gamma}$, thus showing that $\delta\Delta_L \sim \sqrt{\Delta_{0,L}/\Gamma}$ at the Higgs resonance. Thus, the Higgs-enhanced $2\omega_J$ AC Josephson effect can be made arbitrarily strong with decreasing Γ .

D. Susceptibility

Here we look at the susceptibility which governs the magnitude of the OP response for any given frequency and wavevector. The susceptibility is written as,

$$\chi_{\Delta\Delta}(\omega, q_x) = \frac{1}{\frac{1}{g} + \frac{1}{2} \frac{\chi_{\Delta\Delta,0}(\omega, q_x) - \chi_{\Delta\Delta,0}^*(-\omega, -q_x)}{2i}} = \frac{1}{\frac{1}{g} + \frac{1}{2} \Im \chi_{\Delta\Delta,0}(\omega, q_x) - \frac{i}{2} \Re \chi_{\Delta\Delta,0}(\omega, q_x)}, \quad (\text{S8})$$

$$\chi_{\Delta\Delta,0}(\omega, q_x) = \int \frac{d\bar{\omega}}{2\pi} \int \frac{d\mathbf{k}}{(2\pi)^2} \mathbf{tr} [\tau_1 (g_L(\bar{\omega} + \omega; \mathbf{k} + q_x) \tau_1 g_L(\bar{\omega}; \mathbf{k}))^<]. \quad (\text{S9})$$

In the second equality of Eq. (S8), we need to substitute the BCS coupling constant g by obtaining its value from the zero-temperature equilibrium gap equation,

$$\Delta_0 = \Re \frac{ig}{2} \mathbf{tr} [\tau_1 g_L^<(t, t; x, x)] = \Re ig \int \frac{d\omega}{2\pi} \frac{d\mathbf{k}}{(2\pi)^2} i \underbrace{\frac{\mathbf{tr} [\tau_1 (-2\Im g^r)]}{2}}_{A_s(\omega, k)} f(\omega). \quad (\text{S10})$$

where $k = |\mathbf{k}|$. Using the retarded Green's function,

$$g^r(\omega, k) = \int \frac{d\omega'}{2\pi} \frac{A(\omega', k)}{\omega - \omega' + i\Gamma}, \quad g^<(\omega, k) = -(g^r(\omega, k) - g^a(\omega, k))f(\omega), \quad (\text{S11})$$

$$A(\omega, k) = 2\pi \begin{bmatrix} u_k^2 \delta(\omega - E_k) + v_k^2 \delta(\omega + E_k) & u_k v_k \delta(\omega - E_k) - u_k v_k \delta(\omega + E_k) \\ u_k v_k \delta(\omega - E_k) - u_k v_k \delta(\omega + E_k) & v_k^2 \delta(\omega - E_k) + u_k^2 \delta(\omega + E_k) \end{bmatrix}, \quad \begin{pmatrix} u_k(v_k) = \sqrt{\frac{1}{2} + (-)\frac{\xi_k}{2E_k}} \\ E_k = \sqrt{\xi_k^2 + \Delta_0^2} \end{pmatrix}, \quad (\text{S12})$$

where $\xi_k = \epsilon_k - \mu = -2\zeta \cos(k) - \mu$. Thus, we obtain,

$$\frac{1}{g} = \frac{\nu}{2} \int_{-\infty}^0 d\xi \frac{1}{\sqrt{\Delta_0^2 + \xi^2}} \frac{2 \tan^{-1} \left(\frac{\sqrt{\Delta_0^2 + \xi^2}}{\Gamma} \right)}{2\pi}, \quad (\text{S13})$$

where we have used the wideband limit with a constant density of states ν at the Fermi level.

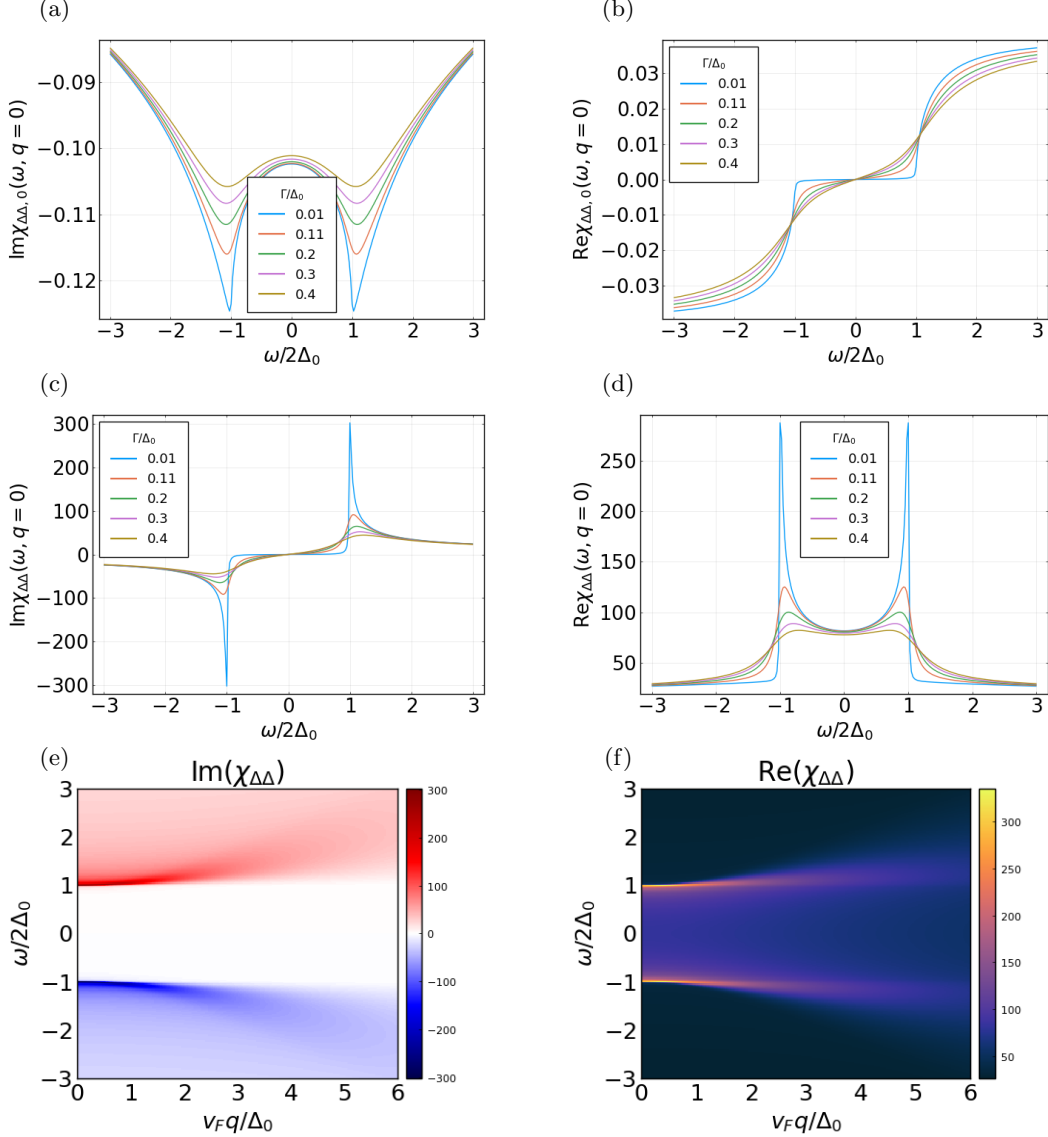


FIG. S1. Pair susceptibility in a system with $\zeta = 20\Delta_0$, $\mu = 0$ (half-filled). (a,b) show $\chi_{\Delta\Delta,0}(\omega, q)$ as a function of frequency ω for $q = 0$, for varying Γ . The $q = 0$ Higgs mode occurs at $\omega/(2\Delta_0) = \pm 1$. (c,d) show the full susceptibility $\chi_{\Delta\Delta}(\omega, q = 0)$, for varying Γ . The singularity in $\chi_{\Delta\Delta}$ at $\omega = \pm 2\Delta_0$ gets stronger with decreasing Γ . (e-f) show the full susceptibility $\chi_{\Delta\Delta}(\omega, q = \xi/v_F)$ for $\Gamma/\Delta_0 = 0.1$, revealing the Higgs dispersion. We state q in terms of the single-particle dispersion $\xi = v_F q$, linearised near the Fermi energy with the Fermi velocity v_F .

In the expression for $\chi_{\Delta\Delta,0}$, the lesser component of the product of Green's functions is obtained using the Langreth rules, as performed previously for δG . $\chi_{\Delta\Delta,0}$ is shown in Fig. S1(a-b), revealing the Higgs mode dispersion. Its $q = 0$ expression can be analytically derived. We define θ as the angle between the internally-summed wavevector \mathbf{k} and the external q , $E_k = \sqrt{\xi_k^2 + \Delta_0^2} := \sqrt{\xi^2 + \Delta_0^2}$ where $\xi = \xi_k = v_F(k - k_F)$ with $k = |\mathbf{k}|$, and $E_{k+q_x} = \sqrt{\xi_{k+q_x}^2 + \Delta_0^2} \approx \sqrt{(\xi + v_F q_x)^2 + \Delta_0^2}$ where $x = \cos(\theta)$. Here we expect the dominant contribution to come from $q_x \ll k_F$ and $k \sim k_F$, with $k_F \approx 2\zeta/v_F$ being the Fermi wavevector. Hence we approximate the otherwise energy-dependent density of states

with its value at the Fermi level. Thus, we get

$$\begin{aligned}
\chi_{\Delta\Delta,0}(\omega, q_x) = & \nu \int_0^\infty d\xi \int_{-1}^1 dx \int_{-\infty}^\infty \frac{d\Omega}{2\pi} (2i\Gamma) \\
& \left[\frac{u_k'^2 u_k^2}{(\Omega + \omega - E_k' + i\Gamma)((\Omega + E_k)^2 + \Gamma^2)} + \frac{v_k'^2 v_k^2}{(\Omega + \omega - E_k' + i\Gamma)((\Omega + E_k)^2 + \Gamma^2)} - \frac{2u_k' v_k' u_k v_k}{(\Omega + \omega - E_k' + i\Gamma)((\Omega + E_k)^2 + \Gamma^2)} \right. \\
& + \frac{v_k'^2 u_k^2}{(\Omega + \omega + E_k' + i\Gamma)((\Omega + E_k)^2 + \Gamma^2)} + \frac{u_k'^2 v_k^2}{(\Omega + \omega + E_k' + i\Gamma)((\Omega + E_k)^2 + \Gamma^2)} + \frac{2u_k' v_k' u_k v_k}{(\Omega + \omega + E_k' + i\Gamma)((\Omega + E_k)^2 + \Gamma^2)} \\
& + \frac{v_k'^2 v_k^2}{((\Omega + \omega + E_k')^2 + \Gamma^2)(\Omega - E_k - i\Gamma)} + \frac{u_k'^2 u_k^2}{((\Omega + \omega + E_k')^2 + \Gamma^2)(\Omega - E_k - i\Gamma)} - \frac{2u_k' v_k' u_k v_k}{((\Omega + \omega + E_k')^2 + \Gamma^2)(\Omega - E_k - i\Gamma)} \\
& \left. + \frac{v_k'^2 u_k^2}{((\Omega + \omega + E_k')^2 + \Gamma^2)(\Omega + E_k - i\Gamma)} + \frac{u_k'^2 v_k^2}{((\Omega + \omega + E_k')^2 + \Gamma^2)(\Omega + E_k - i\Gamma)} + \frac{2u_k' v_k' u_k v_k}{((\Omega + \omega + E_k')^2 + \Gamma^2)(\Omega + E_k - i\Gamma)} \right]. \tag{S14}
\end{aligned}$$

where $E_k' = E_{|\mathbf{k}+q_x|}$ and $u_k'(v_k') = u_{|\mathbf{k}+q_x|}(v_{|\mathbf{k}+q_x|})$. Note that $\chi_{\Delta\Delta}$ depends only on the magnitude of q_x in isotropic s-wave SCs, which is what we consider in this work. On performing the integral over ω , we obtain

$$\begin{aligned}
\chi_{\Delta\Delta,0}(\omega, q_x) = & \nu \int_0^\infty d\xi \int_{-1}^1 dx \int_{-\infty}^\infty i \left[\frac{u_k'^2 u_k^2}{(\omega - E_k - E_k' + i2\Gamma)} + \frac{v_k'^2 v_k^2}{(\omega - E_k - E_k' + i2\Gamma)} - \frac{2u_k' v_k' u_k v_k}{(\omega - E_k - E_k' + i2\Gamma)} \right. \\
& + \frac{v_k'^2 u_k^2}{(\omega - E_k + E_k' + i2\Gamma)} + \frac{u_k'^2 v_k^2}{(\omega - E_k + E_k' + i2\Gamma)} + \frac{2u_k' v_k' u_k v_k}{(\omega - E_k + E_k' + i2\Gamma)} \\
& + \frac{v_k'^2 v_k^2}{(-\omega - E_k - E_k' - i2\Gamma)} + \frac{u_k'^2 u_k^2}{(-\omega - E_k - E_k' - i2\Gamma)} - \frac{2u_k' v_k' u_k v_k}{(-\omega - E_k - E_k' - i2\Gamma)} \\
& \left. + \frac{v_k'^2 u_k^2}{(-\omega + E_k - E_k' - i2\Gamma)} + \frac{u_k'^2 v_k^2}{(-\omega + E_k - E_k' - i2\Gamma)} + \frac{2u_k' v_k' u_k v_k}{(-\omega + E_k - E_k' - i2\Gamma)} \right] \tag{S15}
\end{aligned}$$

For $q_x = 0$, there exists a compact analytical expression,

$$\begin{aligned}
\chi_{\Delta\Delta,0}(\omega, q_x = 0) = & i\nu \int_0^\infty d\xi \int_{-1}^1 dx \frac{4\xi^2}{\sqrt{\xi^2 + \Delta_0^2}((\omega + i2\Gamma)^2 - 4\xi^2 - 4\Delta_0^2)} \\
& \frac{\tanh^{-1} \left(\sqrt{1 + \frac{1}{\left(\frac{\omega}{2\Delta_0}\right)^2 - 1 + i\left(\frac{\omega}{2\Delta_0}\right)\left(\frac{\Gamma}{\Delta_0}\right)}} \right)}{\sqrt{1 + \frac{1}{\left(\frac{\omega}{2\Delta_0}\right)^2 - 1 + i\left(\frac{\omega}{2\Delta_0}\right)\left(\frac{\Gamma}{\Delta_0}\right)}}}. \tag{S16}
\end{aligned}$$

The first term is $i(2/g)$, which is evident from Eq. (S13). It eventually cancels the logarithmic UV divergence in the denominator of $\chi_{\Delta\Delta}$. $\Re\chi_{\Delta\Delta,0}(\omega, q = 0)$, which governs the lifetime of the Higgs mode (see Eq. (S8)), is bounded. It is exponentially small for $|\Omega| < 2\Delta_0$ and satisfies $\Re\chi_{\Delta\Delta,0}(\omega \gg 2\Delta_0, q = 0) = \nu(\pi/2)$ and $\Re\chi_{\Delta\Delta,0}(\omega \ll -2\Delta_0, q = 0) = -\nu(\pi/2)$. $(1/2)\Im\chi_{\Delta\Delta,0}(\omega, q = 0) + (1/g)$ shows a dip at $\omega = \pm 2\Delta_0$, touching zero for $\Gamma/\Delta_0 \rightarrow 0$.

$$\chi_{\Delta\Delta,0}(\omega = 2\Delta_0, q_x = 0) \approx i \left(-\frac{2}{g} + \nu \frac{\pi}{2} \sqrt{\frac{\Gamma}{\Delta_0}} \right) + \left(\nu \frac{\pi}{2} \sqrt{\frac{2\Gamma}{\Delta_0}} - 4\nu \frac{\Gamma}{\Delta_0} \right). \tag{S17}$$

Hence, from Eqs. (S8), (S17), and (S13), $\chi_{\Delta\Delta}$ derives its singular enhancement from that of $\chi_{\Delta\Delta,0}$ at the Higgs resonance,

$$\chi_{\Delta\Delta}(\omega = 2\Delta_0, q_x = 0) \approx \frac{1}{\nu \frac{\pi}{4} \sqrt{\frac{\Gamma}{\Delta_0}} - i \left(\nu \frac{\pi}{4} \sqrt{\frac{\Gamma}{\Delta_0}} - 2\nu \frac{\Gamma}{\Delta_0} \right)} \tag{S18}$$

E. Source

Considering a two-dimensional system (planar junction), from Eq. (9), the expression for the source s_ϕ in time and space domain is given by,

$$s_\phi(t; \{x, y\}) = -\frac{1}{2} \Im \iint_{t_1, t_2} \sum_{y_1, y_2} \mathbf{tr} [\tau_1 g_L(t, t_1; \{x, y\}, \{0, y_1\}) \Sigma_{T,LR}(t_1) g_R(t_1, t_2; \{0, y_1\}, \{0, y_2\}) \Sigma_{T,RL}(t_2) g_L(t_2, t; \{0, y_2\}, \{x, y\})]^\prec. \quad (\text{S19})$$

On Fourier transforming, denoting $N_{x,y}$ the number of sites along the x, y directions,

$$s_\phi(t; \{x, y\}) = -\frac{1}{2} \Im \frac{\sum_{k_{1,x}, k_{2,x}, k_{3,x}, k_{3,y}}}{N_x^3 N_y} \int \frac{d\Omega_1 d\Omega_2 d\omega_3}{(2\pi)^3} \mathbf{tr} [\tau_1 g_L(\omega_3 + \Omega_1 + \Omega_2; k_{1,x}, k_{3,y}) \Sigma_{T,LR}(\Omega_1) g_R(\omega_3 + \Omega_2; k_{2,x}, k_{3,y}) \Sigma_{T,RL}(\Omega_2) g_L(\omega_3; k_{3,x}, k_{3,y})] e^{-i(\Omega_1 + \Omega_2)t + i(k_{1,x} - k_{3,x})x + ik_{3,y}y}, \quad (\text{S20})$$

$$\implies s_\phi(\omega; q_x, 0) = -\frac{1}{2} \frac{\sum_{k_{2,x}, k_{3,x}}}{N_x^2} \int \frac{d\Omega_2 d\omega_3}{(2\pi)^2} \mathbf{tr} [\tau_1 g_L(\omega_3 + \omega; k_{3,x} + q_x, 0) \Sigma_{T,LR}(\omega - \Omega_2) g_R(\omega_3 + \Omega_2; k_{2,x}, 0) \Sigma_{T,RL}(\Omega_2) g_L(\omega_3; k_{3,x}, 0)]. \quad (\text{S21})$$

The tunneling self energy $\Sigma_{T,LR/RL}(\Omega) = -\mathcal{T} \begin{bmatrix} \delta(\Omega \mp eV) & 0 \\ 0 & -\delta(\Omega \pm eV) \end{bmatrix}$ is dimensionless. Due to this form for $\Sigma_{T,LR/RL}(\Omega)$, s_ϕ only has terms which oscillate with frequency $\pm\omega_J = \pm 2eV$ and a DC term. Note that this DC component is neglected in the phenomenological model in the introduction of the main text.

F. Current

Here we derive the leading order change in the current due to the Higgs oscillations of the OP.

$$I(t) = -2e\Re \mathbf{Tr} [\tau_3 \Sigma_{LR}^T \underbrace{(g_R \Sigma_{RL}^T g_L)^\prec}_{(\delta G_{R,L}^\prec)^{(1)}}(t, t)] = -2eh_0(t), \quad (\text{S22})$$

where

$$h_0(t) = \Re \int dt_1 \mathbf{tr} \left[\tau_3 \Sigma_{LR}^T(t) (g_R(t - t_1, 0 - 0) \Sigma_{RL}^T(t_1) g_L(t_1 - t, 0 - 0))^\prec \right]. \quad (\text{S23})$$

In order to align with the simple approximation employed in the introduction of the main text, we have to consider the ‘‘adiabatic’’ approximation [S3] wherein the time-correlators are forced to be local. For a subgap ($eV < 2\Delta$) DC voltage bias with $\phi(t) = 2eVt$, this yields [S3],

$$I = J_1 \Delta_{0,R} \Delta_{0,L} \sin(2eVt) + J_2 \Delta_{0,R} \Delta_{0,L} \cos(2eVt). \quad (\text{S24})$$

Note the cosine term, which is typically omitted in the simple version as it is typically not relevant for $eV < 2\Delta$, and it doesn’t change our conclusions.

The change in the current due to the Higgs oscillations is subsequently obtained as,

$$\delta I(t) = -2e\Re \mathbf{Tr} [\tau_3 \Sigma_{LR}^T \underbrace{(g_R \Sigma_{RL}^T g_L \Sigma_{\delta\Delta_L} g_L)^\prec}_{(\delta G_{R,L}^\prec)^{(2)}}(t, t)] = -2e \int_{-\infty}^t dt' h(t, t'; x') \delta\Delta_L(t', x'), \quad (\text{S25})$$

where,

$$h(t, t'; x') = \left. \frac{\partial h_0(t)}{\partial \Delta_L(t', x')} \right|_{\Delta_L(t', x') = \Delta_{0,L}} \quad (\text{S26})$$

$$= \Re \int dt_1 \mathbf{tr} \left[\tau_3 \Sigma_{LR}^T(t) (g_R(t - t_1, 0 - 0) \Sigma_{RL}^T(t_1) g_L(t_1 - t', 0 - x') \tau_1 g_L(t' - t, x' - 0))^\prec \right]. \quad (\text{S27})$$

The function h inherits the spatio-temporal decay from the Green's functions. That is, as a function of $t - t'$, it decays over a time-scale governed by $1/\Gamma$, whereas as a function of x' , it decays over a length-scale governed by $\xi_{sc,L}$, the superconducting coherence of the left lead. Physically speaking, the current at the junction depends on the OP variation $\delta\Delta(t'; x')$ in the region of space-time limited by these.

Within the adiabatic approximation, using the derivative form specified above and assuming that $\delta\Delta$ is peaked near the junction, we find

$$\delta I \sim J_1 \Delta_{0,R} \delta\Delta_L \sin(2eVt) + J_2 \Delta_{0,R} \delta\Delta_L \cos(2eVt), \quad (\text{S28})$$

which is the expression employed in the introduction. The cosine term is neglected in the main text for reasons mentioned above.

S2. NUMERICAL ANALYSIS

A. Varying junction coupling

As mentioned in the main text, the signatures of the Higgs resonance, $\delta\Delta$ oscillating at frequency ω_J and the consequent $2\omega_J$ AC Josephson current, get stronger with increasing \mathcal{T} . Consequently, for larger values of \mathcal{T} , we can obtain a dominant $2\omega_J$ current with smaller equilibrium gap asymmetry. For large values of \mathcal{T} , such as between $0.3\zeta - 0.4\zeta$ in Fig. S2, we see that the ω_J current decreases in magnitude while the $2\omega_J$ current grows. This arises as the equilibrium DC gap is depleted near the junction, with the electrons now increasingly participating in forming the Higgs-oscillating pairs.

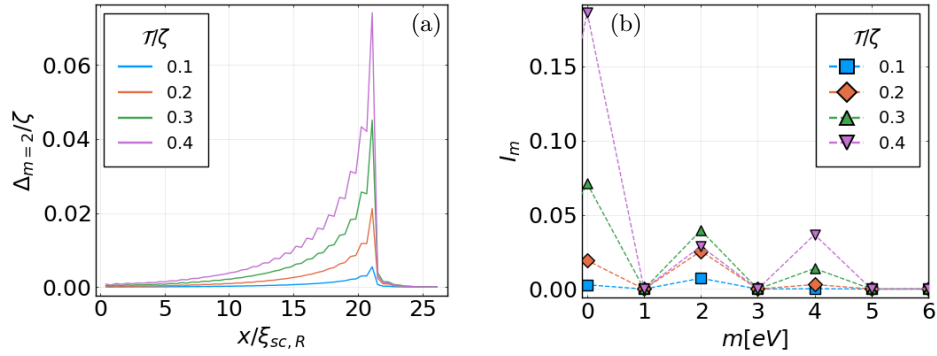


FIG. S2. Numerically obtained results for varying \mathcal{T} , while keeping $\Delta_{0,L/R}$ constant. We consider the same parameters as Fig. 2, but with $\Delta_{0,L}/\Delta_{0,R} = 0.052$. With increasing \mathcal{T} , both (a) Δ_2 (frequency $\omega_J = 2(eV)$), and (b) I_4 (frequency $2\omega_J = 4(eV)$) strengthen. In (b), we find that for $\mathcal{T}/\zeta = 0.4$ (normal state transparency ≈ 0.48 [S4]), the $2\omega_J$ current I_4 is larger than the usual ω_J current I_2 .

B. Varying hopping/bandwidth

Here we present results with varying ζ (bandwidth = 4ζ), keeping the equilibrium gap $\Delta_{0,L/R}$ unchanged. We ensure that the junction transparency remains constant which amounts to fixing \mathcal{T}/ζ [S4]. To understand this, we first consider the current flowing between two normal metallic leads [S5],

$$I = \frac{2e}{\hbar} \int_{-\infty}^{\infty} d\omega \mathbb{T}(\omega, V) [f(\omega - eV) - f(\omega)] \xrightarrow{\text{Zero temperature}} \frac{2e}{\hbar} \int_0^{eV} d\omega \mathbb{T}(\omega, V), \quad (\text{S29})$$

$$\mathbb{T}(\omega, V) \approx \frac{4(\frac{\mathcal{T}}{\zeta})^2}{(1 + (\frac{\mathcal{T}}{\zeta})^2)^2}, \quad (\text{S30})$$

where an approximate result for the transparency $\mathbb{T}(\omega, V)$ is presented in the second line, which is valid near the Fermi level for $eV \ll \zeta$. To keep the current unchanged with changing bandwidth ζ , one must keep \mathcal{T}/ζ constant. Physically

speaking, the transparency (defined in terms of the internal high energy hopping/bandwidth parameter) is a low-energy parameter which governs the low-energy transport properties. Furthermore, it constitutes the small/perturbative parameter for the perturbative expansion of the current. On scaling the tunnel coupling similarly as the hopping ζ , electrons at the junction perceive the same barrier. Otherwise, we eventually end up in the tunnel limit with increasing bandwidth. By this scheme for keeping the transparency fixed, we show that the smallness of Δ_0/ζ (typical of conventional superconductors), which does shrink with increasing bandwidth as we keep Δ_0 fixed, does not affect our conclusions qualitatively. Instead, the dominance of the Higgs-induced AC Josephson current depends primarily on a sufficiently high junction transparency.

We find that with increasing ζ , Δ_2 (the component of the OP oscillating at ω_J) becomes stronger, which results in a larger $2\omega_J$ current. First, we show this analytically by obtaining the scaling of the source and the susceptibility (derived in the previous section) with varying ζ . We start with the expression for the non-equilibrium OP obtained in Eq. (S5). Each of the Green's functions have dimensions $\sim 1/\omega$, and specifically, they scale as $\sim 1/\zeta$. That is, ζg_L has the same magnitude regardless of ζ . This is easy to see on realising that the spectral function bears the same functional shape for BCS superconductors regardless of ζ , and but are spread out over a region of bandwidth $\sim \zeta$. Also, $\delta\Delta(\omega, \mathbf{q})$ is dimensionless, the BCS coupling g has dimensions $\sim \omega$, and $\Sigma_{T,LR/RL}(\Omega) = -\mathcal{T} \begin{bmatrix} \delta(\Omega \mp eV) & 0 \\ 0 & -\delta(\Omega \pm eV) \end{bmatrix}$ is dimensionless. Thus, both the numerator and denominator in Eq. (S5) have dimensions $\sim 1/\omega$. We scale all energies/frequencies ($\hbar = 1$) by $\Delta_{0,L}$ and denote the scaled quantities by tilde. We also define the dimensionless $\tilde{g} = \zeta g$, and $\Sigma_{T,LR/RL}(\Omega) = -\mathcal{T}(1/\Delta_{0,L}) \begin{bmatrix} \delta(\tilde{\Omega} \mp e\tilde{V}) & 0 \\ 0 & -\delta(\tilde{\Omega} \pm e\tilde{V}) \end{bmatrix} = -\tilde{\mathcal{T}}\tilde{\Sigma}_{T,LR/RL}(\tilde{\Omega})$. Also, from the previous section, the susceptibility $\chi_{\Delta\Delta,L} \sim 1/\nu$, where $\nu \sim 1/\zeta$. So, we define $\chi_{\Delta\Delta,L} = \zeta\tilde{\chi}_{\Delta\Delta,L}$ where the dimensionless $\tilde{\chi}_{\Delta\Delta,L} \sim \sqrt{\Gamma/\Delta_{0,L}}$ at the Higgs resonance. $s_{\phi,L}(\omega, q_x)$ in the numerator of Eq. (S5) becomes,

$$s_{\phi,L}(\omega, q_x) = \frac{\mathcal{T}^2}{\zeta^3} \left(-\frac{1}{2} \sum_{k_{2,x}, k_{3,x}} \int \frac{d\tilde{\Omega}_2 d\tilde{\omega}_3}{(2\pi)^2} \mathbf{tr} [\tau_1 \tilde{g}_L(\tilde{\omega}_3 + \tilde{\omega}; k_{3,x} + q_x, 0) \tilde{\Sigma}_{T,LR}(\tilde{\omega} - \tilde{\Omega}_2) \tilde{g}_R(\tilde{\omega}_3 + \tilde{\Omega}_2; k_{2,x}, 0) \tilde{\Sigma}_{T,RL}(\tilde{\Omega}_2) \tilde{g}_L(\tilde{\omega}_3; k_{3,x}, 0)] \right). \quad (\text{S31})$$

The dimensionless quantity inside the parenthesis scales as $(\zeta/\Delta_{0,L})$. This may be checked numerically by substituting the Lehmann representation for the Green's functions, using $\sum_{k_x} \approx \nu \int_{-\zeta}^{\zeta} d\xi$ where $\nu \sim 1/\zeta$ is the density of states at the Fermi level (as shown in the section for the susceptibility), and analysing the integral. Hence, using the scaling of susceptibility obtained above, from Eq. (S5) we find that $\delta\Delta_L(\omega, q_x)$ depends on ζ via the factor $(\mathcal{T}/\zeta)^2 (\zeta/\Delta_{0,L}) \sqrt{\Delta_{0,L}/\Gamma}$. Since we fix the normal state transparency for a fair comparison across varying ζ by holding \mathcal{T}/ζ constant, $\delta\Delta$ increases with ζ . While this result is obtained for two dimensions, it is independent of the number of dimensions on assuming transverse homogeneity and a constant density of states at the Fermi-level (ν).

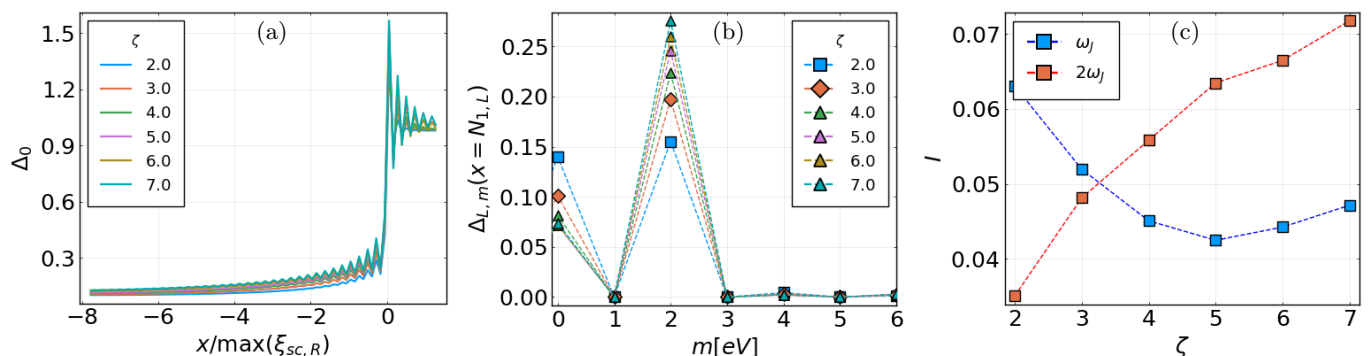


FIG. S3. Numerically obtained results for varying ζ , while keeping $\Delta_{0,L/R}$, eV , and $\mathcal{T}/\zeta = 0.4$ (normal state transparency ≈ 0.48 [S4]) fixed. We consider the same parameters as Fig. 2. (a) The equilibrium gaps Δ_0 . We alter the BCS couplings with ζ suitably to keep the bulk values of Δ_0 unchanged. (b) The Floquet components of the non-equilibrium gap of the left lead $\Delta_{L,m}$ at the site immediately neighbouring the junction at $x = N_{1,L}$. (c) The amplitude (arbitrary units) of the ω_J (blue) and $2\omega_J$ (red) components of the current.

Now, the $\mathcal{O}(\mathcal{T}^2)$ current (without Higgs) given by Eq. (S23) can be written as,

$$I(t) = \left(\frac{\mathcal{T}}{\zeta}\right)^2 \Delta_{0,L} \frac{\sum_{k_{2,x}, k_{4,x}}}{N_x^2} \Re \int \frac{d\tilde{\omega}_1 d\tilde{\omega}_3 d\tilde{\omega}_4}{(2\pi)^3} \mathbf{tr} [\tau_3 \tilde{\Sigma}_{LR}(\tilde{\omega}_1) \tilde{g}_R(\tilde{\omega}_4 + \tilde{\omega}_3; k_{2,x}, k_{2,y}) \tilde{\Sigma}_{RL}(\tilde{\omega}_3) \tilde{g}_L(\tilde{\omega}_4; k_{4,x}, k_{4,y})] e^{-i(\omega_1 + \omega_3)t} \\ \sim \left(\frac{\mathcal{T}}{\zeta}\right)^2 \Delta_{0,L} \quad (S32)$$

where we have used the same scaling conventions as above. Since the scaled self-energies are dimensionless Dirac-delta functions, we only have one integral. On considering a DC voltage bias and expanding the trace to reveal the current component oscillating at ω_J , we find that the integral is independent of ζ . Hence, the ω_J Josephson current, as well as the corresponding DC component, scale as $(\mathcal{T}/\zeta)^2$, which remains unchanged if we fix the transparency, as explained at the beginning of this section. As shown in Ref. [S2], this dependence on $(\mathcal{T}/\zeta)^2$ corresponds to $1/R_N$ where $R_N \sim 1/(\nu^2 \mathcal{T}^2)$ is the normal state resistance.

Similarly, the $\mathcal{O}(\mathcal{T}^4)$ current (with Higgs, $\delta\Delta$ provides the extra \mathcal{T}^2) given by Eq. (S25) is written as,

$$\delta I(t) = \left(\frac{\mathcal{T}}{\zeta}\right)^2 \frac{\Delta_{0,L}^2}{\zeta} \frac{\sum_{k_{2,x}, k_{5,x}, k_{6,x}}}{N_x^3} \Re \int \frac{d\tilde{\omega}_1 d\tilde{\omega}_3 d\tilde{\omega}_5 d\tilde{\omega}_6}{(2\pi)^4} \mathbf{tr} [\tau_3 \tilde{\Sigma}_{LR}(\tilde{\omega}_1) \tilde{g}_R(\tilde{\omega}_3 + \tilde{\omega}_5 + \tilde{\omega}_6; k_{2,x}, 0) \tilde{\Sigma}_{RL}(\tilde{\omega}_3) \\ \tilde{g}_L(\tilde{\omega}_5 + \tilde{\omega}_6; k_{5,x} + k_{6,x}, 0) \tau_1 \delta\Delta_L(\tilde{\omega}_5, k_{5,x}) \tilde{g}_L(\tilde{\omega}_6; k_{6,x})] e^{-i(\omega_1 + \omega_3 + \omega_5)t} \sim \left(\frac{\mathcal{T}}{\zeta}\right)^4 \Delta_{0,L} \left(\frac{\zeta}{\Delta_{0,L}}\right) \sqrt{\frac{\Delta_{0,L}}{\Gamma}}. \quad (S33)$$

We found numerically that the integral (discounting the scaling of $\delta\Delta$) scales as $\sim \zeta/\Delta_{0,L}$. Therefore, its strength relative to the usual Josephson current is obtained as $\delta I/I \sim (\mathcal{T}/\zeta)^2 (\zeta/\Delta_{0,L}) \sqrt{\Delta_{0,L}/\Gamma}$. On fixing the transparency (\mathcal{T}/ζ fixed), the Higgs-enhanced Josephson current is relatively enhanced with respect to the usual Josephson current.

Physically, while the currents depend on the transparency and the applied voltage, for the Higgs-mediated δI there is an additional dependence on the bandwidth arising from the oscillating OP $\delta\Delta$. Since the Higgs oscillations occur microscopically when the pairs coherently dissociate into quasiparticles and recombine, we expect it to depend on the available quasiparticle states above the superconducting excitation gap. This reflects in the Higgs susceptibility scaling as $\sim \zeta$. The source term, at the leading order, must depend on the transparency $(\mathcal{T}/\zeta)^2$ as it is obtained solely due to the junction tunneling processes. Since we keep the voltage and equilibrium gaps fixed, we do not expect any additional dependence on ζ . Thus, we expect that $\delta\Delta$ depends on the bandwidth as $\delta\Delta \sim (\mathcal{T}/\zeta)^2 \zeta$. However, on fixing the transparency for reasons mentioned above, we fix \mathcal{T}/ζ , which translates into a linear dependence $\delta\Delta \sim \zeta$. This causes the Higgs-mediated AC Josephson current to dominate.

Our numerical results (single channel model) are presented in Fig. S3. We observe a small downturn/minimum in the usual ω_J Josephson current, likely arising as the Higgs enhancement $\delta\Delta$ increases with ζ , which reduces the equilibrium gap as the corresponding electrons are now participating more and more in forming the Higgs oscillating pairs instead of static pairs. These effects are not captured by the leading order perturbative analysis.

C. Varying number of transverse modes/sub-bands: Planar specular junctions

In the main text, we consider: (a) junction couplings independent of energy, which is valid for voltages $\sim \Delta$, (b) specular tunneling at the junction, and (c) homogeneity along the transverse direction. Neglecting edge effects, these considerations result in the OP being a function of only the coordinate representing the longitudinal direction parallel to the current transport. In this case, the system splits into disjoint transverse subbands with different chemical potentials, given by the subband energies. As such, for computational simplicity, we performed the calculations in the main text considering only a single-channel model, which is expected to yield qualitatively accurate results. Here we expand upon this, considering a multi-channel system, thereby accounting for finite transverse dimensions.

In Fig. S4, we present results with varying number of transverse modes N_k , corresponding to varying widths of the planar junction. We find that with increasing device width, the difference in strengths of the $2\omega_J$ and ω_J Josephson currents are accentuated, resulting from the contribution from an extensively scaling number of subbands. Crucially, the order of dominance is not affected, i.e., if the $2\omega_J$ current is stronger in the few-channel/subband limit, then it remains stronger even on increasing the device width.

Considering a two-dimensional planar junction, for a given number of sites $N_y = N_k$ along the y -direction (perpendicular to the longitudinal x -direction), the action splits into a disjoint sum of single-channel subbands,

$$S = \sum_k S_{L,k} + S_{R,k} + S_{T,k}, \quad (S34)$$

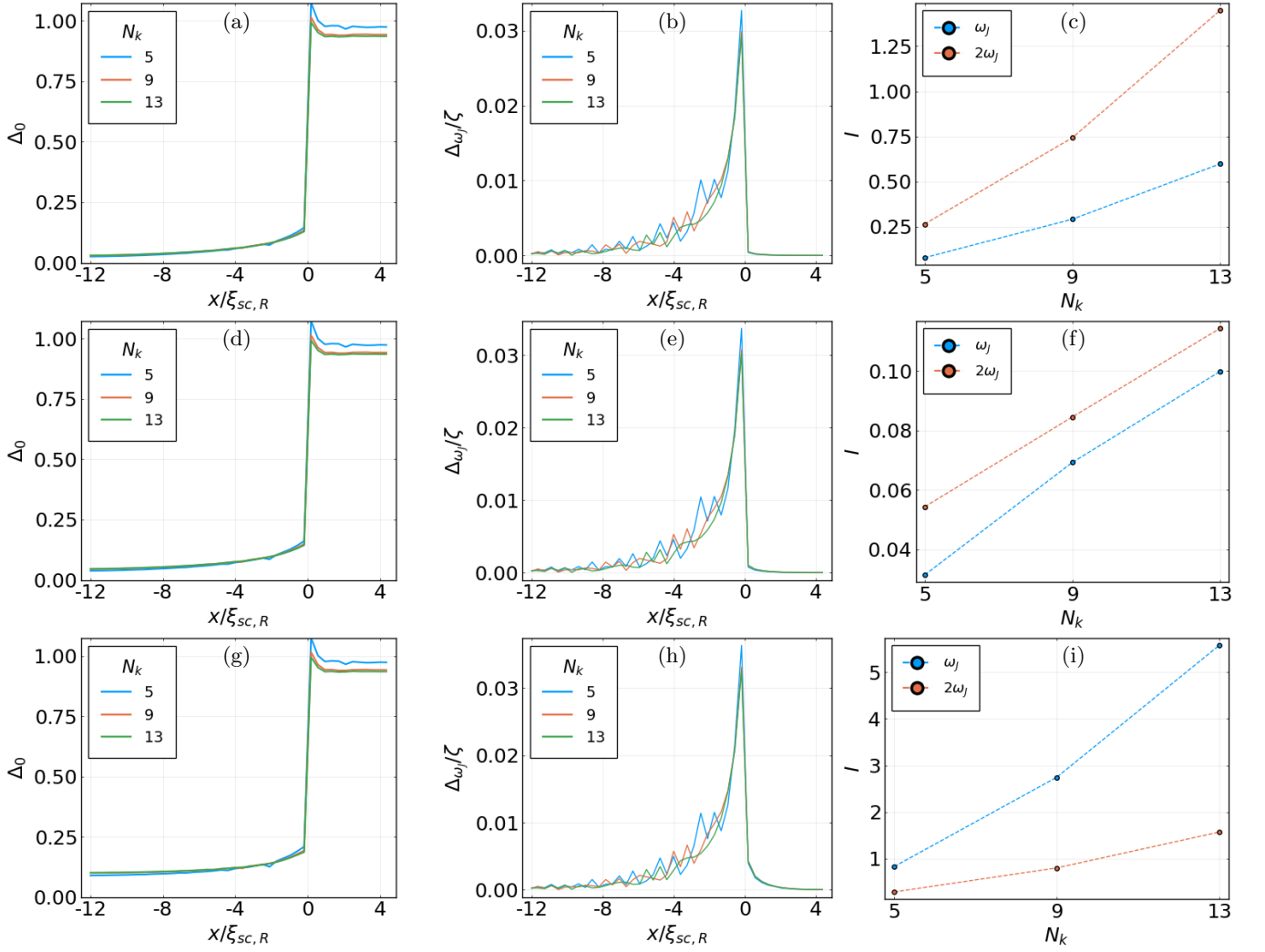


FIG. S4. Numerically obtained results for varying number of transverse modes N_k , while keeping the BCS coupling constant in each lead. We consider the same parameters as Fig. 2, but $g_L/\zeta = 1.35$ and $g_R/\zeta = 2.5$. With increasing N_k , (a) Δ_0 and (b) $\Delta_{m=2} = \Delta_{\omega_J}$ oscillating at frequency $\omega_J = 2(eV)$ acquire limiting values for wide planar junctions which do not change with further increase in N_k . (c) The $2\omega_J = 4eV$ current is larger than the usual $\omega_J = 2eV$ current as N_k increases. (d-f) Same as (a-c), but for $g_L/\zeta = 1.375$ (as opposed to 1.35 in (a-c)) and $g_R/\zeta = 2.5$. In this case, we find that the usual ω_J current dominates. The $2\omega_J$ current is at the threshold of dominating. (g-i) Same as (a-c), but for $g_L/\zeta = 1.44$ (as opposed to 1.35 in (a-c)) and $g_R/\zeta = 2.5$. In this case, we find that the usual ω_J current dominates.

where

$$S_{j=L/R,k} = \sum_{j \in L/R,\sigma} \int_t (-2\zeta \cos(k) c_{j\sigma k}^\dagger c_{j\sigma k}) + (-\zeta c_{j+1\sigma k}^\dagger c_{j\sigma k} - \zeta c_{j\sigma k}^\dagger c_{j+1\sigma k}) + (\Delta_j(t) c_{j\sigma k}^\dagger c_{j\sigma'k}^\dagger + \Delta_j^*(t) c_{j\sigma'k} c_{j\sigma k}) + \frac{\Delta_j(t)^2}{g}, \quad (\text{S35})$$

and

$$S_{T,k} = \sum_{\sigma} \int_t -\mathcal{T} (e^{i\frac{\phi(t)}{2}} c_{LN_{1,L}\sigma k}^\dagger c_{R1\sigma k} + e^{-i\frac{\phi(t)}{2}} c_{R1\sigma k}^\dagger c_{LN_{1,L}\sigma k}). \quad (\text{S36})$$

Here $k \in \{\pi/(N_k + 1), 2\pi/(N_k + 1) \dots N_k\pi/(N_k + 1)\}$, which implements Dirichlet conditions at the sites 0, $N_k + 1$, immediately outside the device consisting of sites 1 through N_k .

Subsequently, recalling that Δ depends only on x ($\Delta_{k_x, k_y} = N_k \delta_{k_y} \Delta_{k_x}$), we self-consistently solve,

$$\begin{aligned} G_k^< &= G_k^r \Sigma^< G_k^a \\ \Delta_{j_x}(t) &= \frac{1}{N_k} \Re \sum_k i g F_{j_x, j_x, k}^<(t, t). \end{aligned} \tag{S37}$$

Finally, the current is obtained using Eq. (8) for each subband, which are then summed up [S1].

* aritra.lahiri@uni-wuerzburg.de

- [S1] J. C. Cuevas and A. L. Yeyati, Phys. Rev. B **74**, 180501 (2006).
- [S2] A. Barone and G. Paterno, Physics and Applications of the Josephson Effect (Wiley, New York, 1982).
- [S3] A. I. Larkin and Y. N. Ovchinnikov, Zh. Eksp. Teor. Fiz. **51**, 1535 [Sov. Phys. JETP **24**, 1035 (1967)].
- [S4] J. C. Cuevas, A. Martín-Rodero, and A. Levy Yeyati, Phys. Rev. B **54**, 7366 (1996).
- [S5] J. C. Cuevas and E. Scheer, Molecular Electronics: An Introduction To Theory And Experiment (World Scientific, Singapore, 2010).